Copy No. _____

Defence Research and Development Canada
Recherche et développement pour la défense Canada

DEFENCE R&D DÉFENSE

VHF Propagation Study

D. Green, C. Fowler and D. Power
C-CORE

J. K. E. Tunaley
London Research and Development Corporation

Prepared by:
C-CORE
1 Morrissey Road
St. John's, NL A1B 3X5

Contractor's Document Number: R-11-020-868
Contract Project Manager: Chris Fowler, 709-864-8373
PWGSC Contract Number: W7707-115279
Contract Scientific Authority: Anna-Liesa Lapinski, Defence Scientist, 902-216-3100 ext. 180

Defence R&D Canada – Atlantic

Contract Report
DRDC Atlantic CR 2011-152
September 2011

Canada

This page intentionally left blank.

VHF Propagation Study

D. Green
C-CORE

J. K. E. Tunaley
London Research and Development Corporation

C. Fowler
C-CORE

D. Power
C-CORE

Prepared By:
C-CORE
1 Morrissey Road
St. John's, NL A1B 3X5

Contractor's Document Number: R-11-020-868
Contract Project Manager: Chris Fowler, 709-864-8373
PWGSC Contract Number: W7707-115279
CSA: Anna-Liesa Lapinski, Defence Scientist, 902-216-3100 ext. 180

Defence R&D Canada – Atlantic

Contract Report
DRDC Atlantic CR 2011-152
September 2011

Principal Author

Original signed by David Green

David Green

C-CORE

Approved by

Original signed by Francine Desharnais

Francine Desharnais

Head, Maritime Information and Combat Systems Section

Approved for release by

Original signed by Ron Kuwahara for

Calvin Hyatt

Chair, Document Review and Library Committee

Abstract

This literature review provides DRDC researchers with information related to the propagation of VHF signals, particularly as it relates to the fluctuating limits of Automatic Identification System (AIS) message reception. The review focuses on the AIS frequency range and the factors that influence signal propagation in Maritime environments. The approach taken was consultation with classical textbooks on propagation to capture fundamental equations, followed by a search of the literature for papers involving VHF propagation of AIS signals. Three effects were determined to most likely extend the range of AIS transmission: diffraction over the sea around the curvature of the earth, ducting resulting from the varying refractivity of air, and multipath effects.

Résumé

La présente revue de littérature fournit aux chercheurs de RDDC des renseignements sur la propagation des signaux VHF, particulièrement en ce qui concerne les limites fluctuantes de réception de messages du Système d'identification automatique (AIS). Elle porte surtout sur la gamme de fréquences de l'AIS et les facteurs qui influencent la propagation des signaux en milieu maritime. L'approche utilisée a consisté à d'abord consulter des manuels classiques sur la propagation afin de relever les équations fondamentales, puis à effectuer des recherches dans les publications scientifiques pour trouver des articles portant sur la propagation des signaux AIS. Ce travail a permis de déterminer que trois effets étendent très vraisemblablement la portée de transmission AIS : la diffraction sur la surface de la mer en raison de la courbure terrestre, la propagation guidée résultant de la variation de l'indice de réfraction de l'air, et les effets des trajets multiples.

This page intentionally left blank.

Executive summary

VHF Propagation Study

D. Green; J. K. E. Tunaley; C. Fowler; D. Power; DRDC Atlantic CR 2011-152; Defence R&D Canada – Atlantic; September 2011.

Introduction: This literature review provides DRDC researchers with information related to the propagation of VHF signals, particularly as it relates to the fluctuating limits of Automatic Identification System (AIS) message reception. The review focuses on the AIS frequency range and the factors that influence signal propagation in Maritime environments.

The approach followed is designed to meet the requirements laid out in the Request for Proposal (RFP) to provide DRDC with information regarding the propagation of VHF signals in Canada's coastal areas. This approach ensures that the literature review is well substantiated and that all supporting information is traceable to reliable sources. The approach was, for the most part, consultation with classical textbooks on propagation to capture fundamental equations, followed by a search of the literature for papers involving VHF propagation of AIS signals (modeling, effects, issues, etc.).

Results: Three primary phenomena were determined to impact AIS transmission. Diffraction over the sea around the curvature of the earth, as well as ducting resulting from a variable refractivity of air, would both potentially extend the transmission range of AIS signals. Multipath causes significant variability in the signal strength. These are the major factors identified in the software implementation of ITU-R (International Telecommunication Union Recommendation) P.452-14, *Prediction procedure for the evaluation of interference between stations on the surface of the Earth at frequencies above about 0.1 GHz*, and hence it is recommended that this implementation be considered for further modelling of VHF propagation effects.

Significance: Using knowledge of the VHF propagation, it is likely possible to predict areas of reliable AIS coverage based on current conditions or forecasted conditions. Reliable AIS reception can be used to indicate areas where a surveillance officer can be assured that broadcast AIS messages are being received reliably. In areas identified as having unlikely coverage, surveillance officers can recognize that not all broadcasting ships in the area will be identified using AIS.

Future plans: Future work could include using the identified factors that influence the temporal variations in AIS coverage to predict AIS coverage.

Sommaire

VHF Propagation Study

D. Green; J. K. E. Tunaley; C. Fowler; D. Power; DRDC Atlantic CR 2011-152; R & D pour la défense Canada – Atlantique; Septembre 2011.

Introduction : La présente revue de littérature fournit aux chercheurs de RDDC des renseignements sur la propagation des signaux VHF, particulièrement en ce qui concerne les limites fluctuantes de réception de messages du Système d'identification automatique (AIS). Elle porte sur la gamme de fréquences de l'AIS et les facteurs qui influencent la propagation des signaux en milieu maritime.

L'approche suivie a été choisie pour répondre aux exigences de la demande de propositions (DP), en vue de fournir à RDDC des renseignements sur la propagation des signaux VHF dans les zones côtières du Canada. Cette approche permet de veiller à ce que la revue de littérature soit bien justifiée et que l'origine de toute l'information donnée en appui puisse être attribuée à des sources fiables. En somme, l'approche a consisté à d'abord consulter des manuels classiques sur la propagation afin de relever les équations fondamentales, puis à effectuer des recherches dans les publications scientifiques pour trouver des articles portant sur la propagation des signaux AIS (modélisation, effets, questions, etc.)

Résultats : Les travaux effectués ont permis de déterminer que trois principaux phénomènes influent sur les transmissions AIS. La diffraction sur la surface de la mer en raison de la courbure terrestre ainsi que la propagation guidée résultant de la variation de l'indice de réfraction de l'air pourraient toutes deux étendre la portée des signaux AIS. Les trajets multiples créent une variabilité appréciable de l'intensité des signaux. Il s'agit des principaux facteurs distingués dans l'implémentation logicielle de la recommandation de l'Union internationale des télécommunications P.452-14, intitulée *Prediction procedure for the evaluation of interference between stations on the surface of the Earth at frequencies above about 0.1 GHz [Procédure de prédiction pour l'évaluation du brouillage entre des stations sur la surface de la Terre à des fréquences au-dessus d'environ 0,1 GHz]*; il est donc recommandé d'envisager l'utilisation de cette implémentation pour la modélisation future des effets de propagation VHF.

Portée : L'utilisation de connaissances sur la propagation VHF pourrait permettre de prédire les zones où la couverture AIS est fiable en fonction des conditions actuelles ou des conditions prévues. Une réception AIS fiable peut servir à indiquer les zones où un officier de surveillance peut être sûr que les messages AIS émis sont reçus de manière fiable. Dans les zones pour lesquelles la couverture est peu probable, les officiers de surveillance peuvent tenir compte du fait que les navires émettant dans la zone ne seront pas tous identifiés par AIS.

Recherches futures : Les recherches futures pourraient utiliser les facteurs qui influencent la variation de la couverture AIS dans le temps en vue de la prédire.

Table of contents

List of figures

List of tables

Introduction

This literature review provides DRDC researchers with information related to the propagation of VHF signals, particularly as it relates to the fluctuating limits of Automatic Identification System (AIS) message reception. The review focuses on the AIS frequency range and the factors that influence signal propagation in Maritime environments.

The primary objective of this study is to conduct a literature review to provide a basis of understanding on the principles of VHF propagation. This was done in the context of AIS signal reception in a Maritime environment. The review provides the scientific literature that forms the basis of understanding VHF signal propagation and highlights information sources that are highly relevant.

A secondary objective of this project is to identify sources that can provide suitable data for use in calculating VHF propagation limits for various geographic regions around the country. Emphasis was given to coastal regions of Canada's Atlantic, Pacific and Arctic oceans.

Literature Review Methodology

The approach followed is designed to meet the requirements laid out in the Request for Proposal (RFP) to provide DRDC with information regarding the propagation of VHF signals in Canada's coastal areas. This approach ensures that the literature review is well substantiated and that all supporting information is traceable to reliable sources. The approach was, for the most part, consultation with classical textbooks on propagation to capture fundamental equations, followed by a search of the literature for papers involving VHF propagation of AIS signals (modeling, effects, issues, etc.).

The initial component of the literature review was to establish a parameter list for a literature search. The parameter list includes a list of keywords parameterized according to subject, paper title and author. The parameter list was initially established in consultation with DRDC; however, it was appended to as the literature search proceeded. For instance, if a relevant article was found due to a keyword search, then the associated author was added to the list of keywords. The parameter list will be maintained in a checklist format to ensure a comprehensive search was completed. From this, key documents will be identified for subsequent analysis and reporting.

Personnel from C-CORE have access to the Queen Elizabeth II Library belonging to Memorial University of Newfoundland. Being within the university's firewall allows access to library resources and online databases, allowing the project team to view full text articles. In particular, personnel are allowed access to the Institute of Electrical and Electronics Engineers (IEEE) Xplore service, which provides the full text of all articles published within the institute. Personnel from London Research and Development Corporation (LRDC) have access to the library system at the University of Western Ontario for the purposes of research, subject to library regulations and copyright.

AIS Technology

In order to better understand the impacts of the various VHF propagation effects on AIS transmission, it is necessary to review the developments and the fundamentals of AIS technology. The transmission frequencies, multiple access schemes, and signal modulation techniques are all important considerations when evaluating the propagation phenomena outlined in this report.

In 2000, as a part of the Safety Of Life At Sea (SOLAS) regulations, the International Marine Organization (IMO)[1] added Automatic Identification of Ships (AIS) to the shipboard navigational carriage requirement for a number of ship categories. These categories are ships of 300 tons (gross) or greater that travel internationally, cargo ships of 500 tons gross or greater, and all passenger ships. The requirement came into full force for these ships on December 31st 2004 and the system is known as "Class A" AIS. After this date all ships in service in the said categories are mandated to operate their AIS equipment continuously except where international agreements allow navigational data to be protected. In 2007, Class B was introduced for small craft, including pleasure vessels.

AIS was conceived mainly as a collision avoidance system and is based on regular VHF transmission and reception of short binary messages containing information about the ship's identity and includes its position, speed and course. These are "dynamic data". "Static data," such as the ship's name, IMO number, cargo type and estimated time of arrival (ETA) are also transmitted but less frequently. The AIS system is specified in an International Telecommunication Union (ITU) document ITU-R M1371 [1]. The latest version (#4, April 2010) can be found at the ITU site[2] and it is also possible to download the first version, which was published in 1998. AIS systems can also be used for other types of safety related messaging as well as base station interrogations and commands. Another useful document has been published by the International Association of Lighthouse Authorities (IALA); this is IALA Technical Clarifications on Recommendation ITU-R M.1371-1[3].

Reporting rates are specified in ITU-R M1371-4 in Annex 1, Tables 1 and 2. The dynamic data rate varies with ship speed from a minimum of two seconds for Class A (five seconds for Class B) at speeds greater than 23 knots to three minutes for ships at anchor. For the static data a report is transmitted every six minutes. The two VHF bands are also specified in this annex as well as the transmitted power and the modulation type (Gaussian Minimum Shift Keying (GMSK)) and its parameters. Other useful documents specifying GPS and control performances are IMO MSC.74(69) and IMO NAV 48(18).

The AIS systems are based on Time Domain Multiple Access (TDMA). This means that short messages are sent during specific time slots. To avoid confusion when the signal traffic is high, schemes are adopted to ensure that signals are not transmitted simultaneously by different ships into the same time slot. For Class A this is a self-organizing method called Self-Organized Time Domain Multiple Access (SOTDMA). In this method, a transceiver actively searches for an appropriate empty slot before transmitting. For Class B, a transceiver first listens to a slot to

[1] http://www.imo.org/OurWork/Safety/Navigation/Pages/AIS.aspx
[2] http://www.itu.int/rec/R-REC-M.1371/en
[3] e.g. http://www.ialathree.org/iala/pages/AIS/IALATech1.5.pdf

determine if anyone is using it and, if it is free, proceeds to transmit. This is known as Carrier-Sense TDMA (CSTDMA).

Class A messages are divided into various types. The position reports are Types 1, 2 and 3, which contain dynamic data; the static reports are of Type 5. The position reports for Class B messages are Types 18 and 19, while the static report is Type 24. There is also a report designed for long range transmissions to a satellite with an altitude less than 1000 km; this is Type 27. The formats of the reports are defined in terms of bit patterns[4]. These are compact in the sense that the length of a message in bits is minimal.

National governments can add carriage requirements on to those specified by the IMO. The situation in the United States is described on the US Coast Guard Navigation Center website[5].

When AIS is operated as a terrestrial system, the SOTDMA protocols ensure that signals from different ships usually do not interfere with one another. However the number of time slots is limited to 2250 on each of two VHF channels and these slots are reassigned every 60 seconds. Therefore in a very high shipping density, some signals may be dropped. The system is configured so that the weaker signals in the far range are omitted; it results in a reduction of the size of a communications cell and so has little effect on the collision avoidance aspect of the system.

As a collision avoidance system, AIS needs only a line of sight communications system. Therefore the VHF band of frequencies is ideal for terrestrial use. This often limits the range to about 20 nmi but it can be somewhat greater under favourable propagation conditions, such as ducting. The limitation in range implies that the number of ships in the field of view of the antenna that can be accommodated by the AIS scheme is sufficiently small to avoid interference. The typical range can be estimated from the heights of the antennas, $h_{1,2}$, by assuming that the troposphere has its average properties. This latter condition corresponds to setting the radius of the earth to 4/3 of its true value. Therefore, according to simple geometry the typical line of sight range, R, is given in kilometres by (e.g. [2]):

$$R = 4.131 \times \left(h_1^{1/2} + h_2^{1/2} \right) \tag{1}$$

Unfortunately the implementation of AIS is subject to error. Some of the errors made in setting up the ship-board systems are discussed in [3]. For example in various studies, the Maritime Mobile Service Identity (MMSI) number was incorrect 2% of the time and some authors claim that up to 80% of the AIS setups contained at least one error, though this is usually minor.

SOLAS

The Class A and Class B reporting intervals are provided in Table 1 and Table 2. The transmission parameters in section 3.2 are a result of these specifications.

[4] http://www.navcen.uscg.gov/?pageName=AISMessagesBA
[5] http://www.navcen.uscg.gov/

Table 1: Class A Shipborne Mobile Equipment Reporting Intervals

Ship's dynamic conditions	Nominal reporting interval
Ship at anchor or moored and not moving faster than 3 knots	3 min
Ship at anchor or moored and moving faster than 3 knots	10 s
Ship 0-14 knots	10 s
Ship 0-14 knots and changing course	3 1/3 s
Ship 14-23 knots	6 s
Ship 14-23 knots and changing course	2 s
Ship > 23 knots	2 s
Ship > 23 knots and changing course	2 s

Table 2: Reporting Intervals for Equipment Other than Class A Shipborne Mobile Equipment

Platform's condition	Nominal reporting interval
Class B "SO*" shipborne mobile equipment not moving faster than 2 knots	3 min
Class B "SO" shipborne mobile equipment moving 2-14 knots	30 s
Class B "SO" shipborne mobile equipment moving 14-23 knots	15 s
Class B "SO" shipborne mobile equipment moving > 23 knots	5 s
Class B "CS**" shipborne mobile equipment not moving faster than 2 knots	3 min
Class B "CS" shipborne mobile equipment moving 2-14 knots	30 s
Search and rescue aircraft (airborne mobile equipment)	10 s
Aids to navigation	3 min
AIS base station	10 s
* SO = Self-organized ; ** CS = carrier sense	

Signal Specifications

The important parameters specified in [1] for AIS transmissions are provided in Table 3.

Table 3: AIS Transmission Parameters

Parameter	Value
Frequency AIS-1 (MHz)	161.975
Frequency AIS-2 (MHz)	162.025
Bit rate (bits/sec)	9600
Line code	NRZI[6]
Modulation	GMSK[7]
Number of training bits	24
Transmit Bandwidth Time Product	≈0.4
Receive Bandwidth Time Product	≈0.5
Class A Transmitter Power (W)	12.5
Channel bandwidth (kHz)	25

The following message types in Table 4 are relevant to the principal reports of interest. The reports are 256 bits long and, with the exception of message 27, a string of 24 bits within the message is used as a buffer to accommodate bit stuffing, distance variations, repeater delays and synchronization jitter. Of these 24 bits, 12 bits are allocated to distance delay. Noting that the bit rate is 9600 bits/s, it is easily verified that the delay corresponds to a distance of about 375 km or 202 nmi.

Table 4: Message Report Types (IDs)

Message ID	Description
1	Class A scheduled position report
2	Class A assigned scheduled position report
3	Class A special report; interrogation response
5	Class A static report
18	Class B scheduled position report (cf 1,2,3)
19	Class B extended position report
24	Class B static report
27	Class A long range scheduled position report

Signal Modulation

The AIS signals satisfy several requirements. The bandwidth of the signals is small so that they occupy a minimal part of the VHF spectrum and their sidelobes are also small so as to cause minimal interference with signals in neighbouring channels. To minimize costs, the performance is not sensitive to non-linearities in the system and it is possible to receive the information

[6] Non-Return-to-Zero differential line code; a transition occurs when a logical zero is sent but not a logical one.
[7] Gaussian Minimum Shift Keying.

without regenerating a carrier. These requirements are met by using Gaussian Minimum Shift Keying (GMSK).

There is a hierarchy of modulation schemes but the requirement of lack of sensitivity to non-linearities limits consideration to phase and frequency modulations. The requirement to demodulate the signal without reconstructing a carrier tends to limit the modulation to frequency modulation using a binary shift keying. Differential Phase-Shift Keying (DPSK) would have been an option but the Bit Error Rate (BER) is higher [4]. The current specification requires that the logical data is coded using a Non-Return-to-Zero-Inverted (NRZI) line code and this implies that the data can be detected unambiguously using a simple non-coherent Differential Frequency Shift Keying (DFSK) demodulator. However, the power spectral density of a random signal processed with the NRZI line code does not go to zero at zero frequency. Therefore bit-stuffing is needed to remove the dc component (remove the mean value of the waveform).

A narrow bandwidth suggests continuous phase and Minimum Shift Keying (MSK). At first sight, MSK implies that symbols are transmitted by an up or down shift that introduces or removes exactly one cycle during the time that each symbol is transmitted. This ensures that the phase is continuous and that the signals representing each binary symbol are orthogonal so that they can be recovered easily. If the frequency shift is f_m and the inter-symbol time is T_b, this leads to [4]:

$$f_m T_b = h \tag{2}$$

where h is called the deviation ratio. When $h = 1$, we have Sunde's Frequency Shift Keying (FSK). However, it is possible to reduce the bandwidth by a factor of 2 by setting $h = ½$. In this case neighbouring symbols are not independent but can be grouped in pairs to maintain phase continuity. The signal space diagram that represents MSK now has four message points.

As shown in [4], the error probability for coherent MSK (in which the carrier is reconstructed) is similar to that for Quadrature Phase Shift Keying (QPSK); for Additive White Gaussian Noise (AWGN) it is given by:

$$P_e = \frac{1}{2}\operatorname{erfc}\left(\sqrt{\frac{E_b}{N_0}}\right) \tag{3}$$

where E_b is the signal energy per bit and $N_0/2$ is the two-sided noise spectral density. For example, for the available thermal noise power we have the usual formula:

$$N_0 = kT \tag{4}$$

The complementary error function is given by:

$$\operatorname{erfc}(u) = 1 - \frac{2}{\pi^{1/2}} \int_0^u e^{-z^2}\, dz \tag{5}$$

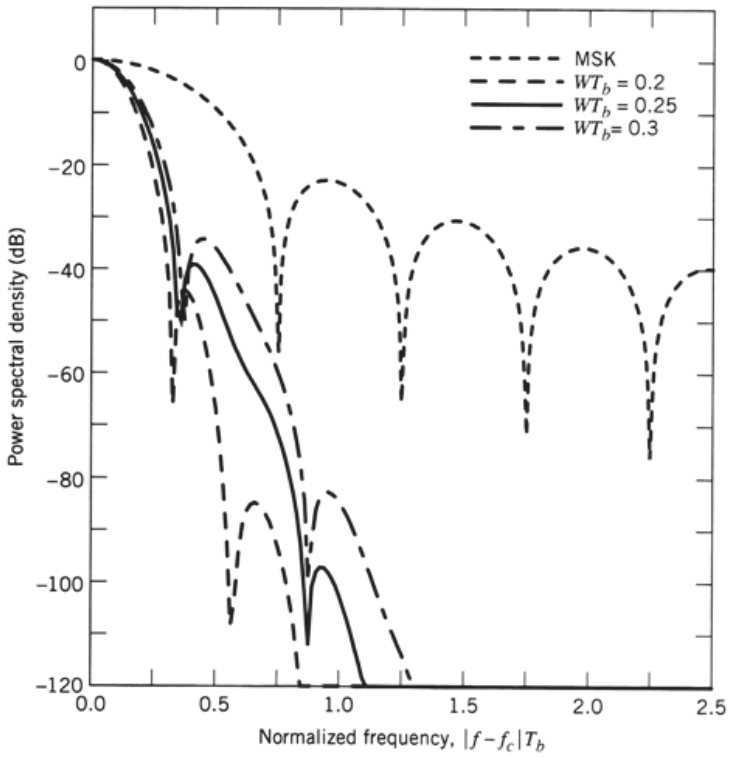

Figure 1: Spectral densities as a function of normalized frequency

The sidelobes of a MSK signal are too large for communications purposes and so the symbol stream is filtered with a Gaussian profile in the frequency domain. This smoothes the modulation and reduces the sidelobes. The spectral densities for various time-bandwidth products are shown in Figure 1. The smoothing is characterized by the time-bandwidth product, WT_b, where W is the 3 dB bandwidth.

The probability of an error is also affected by the Gaussian filtering but the reduction of the bandwidth is not very costly. Again the time-bandwidth product can be employed as a parameter [4] and Figure 2 shows the degradation, D, which is defined in units of decibels as:

$$D = -10 \log_{10}\left(\frac{\alpha}{2}\right) \tag{6}$$

Once the parameter α has been determined from Figure 2 and (6), it can be inserted into a modification of (3):

$$P_e = \frac{1}{2}\operatorname{erfc}\left(\sqrt{\frac{\alpha E_b}{2N_0}}\right) \tag{7}$$

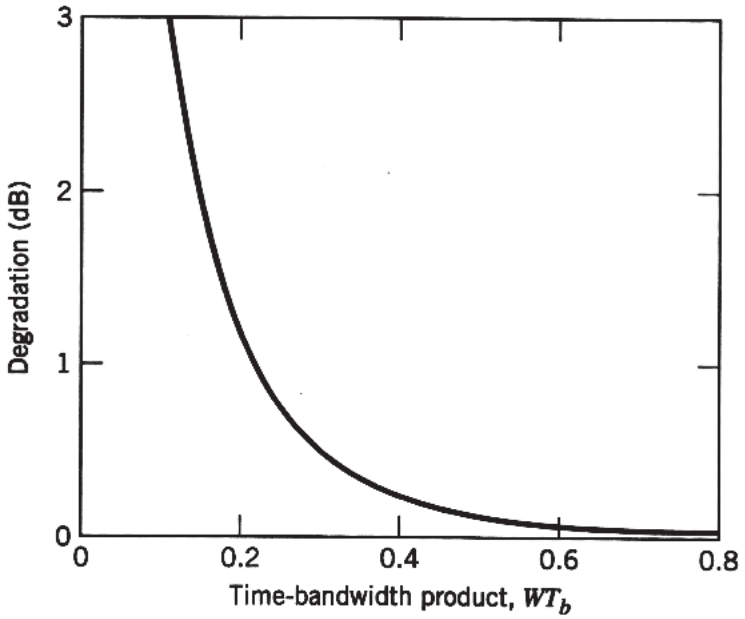

Figure 2: GMSK degradation.

When coherent demodulation cannot be used because of carrier phase jitter, which can be a result of rapid signal fading, non-coherent modulation can be employed. In this case envelope detectors are part of an optimum receiver and there are only two outcomes, either a logical 0 or 1. The probability of a bit error is now given by [4]:

$$P_b = \frac{1}{2}\exp\left(\frac{E_b}{2N_0}\right) \tag{8}$$

For example, if $WT_b = 0.3$, the degradation for coherent demodulation is about 0.46 dB and $\alpha = 1.8$. The BERs for both coherent and (non-differential) non-coherent demodulation for this time-bandwidth product are shown in Figure 3; it is assumed that there is no co-channel interference. The Gaussian filtering makes only a very small difference to the coherent BER. It is obvious that there is a significant advantage in coherent demodulation.

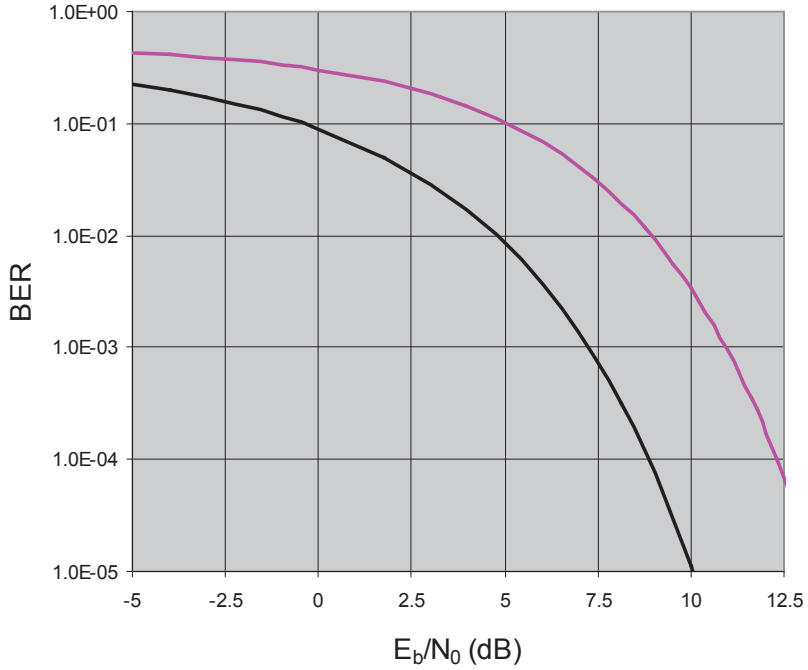

Figure 3: Bit Error Rates for GMSK maximum likelihood coherent demodulation (—) and non-coherent demodulation (—)

Hardware

There are various manufacturers of Class A AIS transponders and receivers, such as CNS Systems of Sweden (ICAN in Canada) and Kongsberg of Norway. The ICAN VDL-6000 transponder is made by CNS and retails for $3800 CAD. This receiver is based on software-defined radio and the unit will be "firmware" up-gradable to accommodate the new AIS channels 3 and 4 designed for space-based AIS. Kongsberg Maritime markets the AIS-200 transponder at a cost of $5355 (includes antenna and GPS antenna). This is also software up-gradable.

There are other versions one of which is portable and another is designed for military blue force operations. In the latter case the AIS messages are encrypted to hide the position information from red forces; the encryption is either Advanced Encryption Standard (AES) or Blowfish.

There are a number of low-end manufacturers and their Class A units are not designed for software up-grade. This is because the receiver front end is based on analog circuitry.

According to one manufacturer, non-coherent DFSK is employed in inexpensive AIS receivers though the BER may be quite poor compared with coherent detection. However, the transponders still meet the ITU specification, which only requires a receiver sensitivity of -107 dBm for a Packet Error Rate (PER) of 20%. This manufacturer has tested various off-the-shelf receivers and found sensitivities ranging from -110 dBm to -114 dBm.

Link Budget

The link budget depends on the transmitter power, path length, antenna gains, cable losses, etc. Table 5 provides notional data based on a free space range of 120 km. This is an extreme terrestrial range and has been chosen to illustrate that large losses can be tolerated.

It has been assumed that the ship-board AIS and the shore based antennas are vertical monopoles or dipoles with some gain towards the horizon. Those channels neighbouring the AIS channels are likely to give rise to low levels of interference and a loss of 4 dB has been assumed. In the far range multi-path propagation is likely to give rise to rapid fading and this has been represented by a further loss of 4 dB. The required Signal to Noise Ratio (SNR) has been set at 12.5 dB. This corresponds to non-coherent demodulation with a BER of 10^{-4}. Non-coherent demodulation would be needed in the presence of heavy rapid fading.

The receiver sensitivity in the table is -107 dBm, which is the minimum specified by the ITU. The result is a large margin of 19.8 dB. This suggests that large additional losses can be tolerated for trans-horizon paths or paths in which obstacles are present and signal losses are associated with diffraction.

Table 5: Class A Link Budget Parameters

Parameter	**Value**
Range (km)	120
Elevation Angle (deg)	0
Transmit Power (W)	12.5
Ship Antenna Gain (dB)	2
Receiver Antenna Gain (dB)	2
Total Cable Losses	6
Interference Loss (dB)	4
Fading Loss (dB)	4
Required SNR (dB)	12.5
Received Power (dBW)	--117.2
Receiver Sensitivity from ITU (dBW)	--137.0
Margin (dB)	19.8

Troposphere Effects on AIS Technology

Several phenomena affecting VHF propagation can be found within the troposphere. Turbulent irregularities in the refractive index can scatter the signal. As the refractive index of air is based on a variety of natural factors, an atmospheric profile results which may cause ducting. Lightning strikes can cause reflections. Precipitation, referred to as hydrometeors, can also attenuate or scatter a signal. All of these phenomena are examined and their effects on VHF propagation, and hence AIS signal transmission, are evaluated.

Tropospheric Scatter

VHF energy can be scattered via small-scale irregularities in the troposphere. These irregularities result from small variations in temperature and humidity from the ambient values. When large scale air masses of differing refractivity move alongside each other, a shear results along the interface [2]. Large eddies on the order of 100 m in size will form because of the turbulent mixing of air at the boundary. These large eddies create increasingly smaller eddies by a similar mechanism, until they approach a size on the order of 1 mm, at which point viscosity counterbalances the effect of the turbulence and the spawning process halts [5].

These eddies can defocus and refocus an impinging radio wave, which manifests itself as rapid amplitude and phase fluctuations. For larger aperture antennas this results in a perceived degradation in antenna gain. However, the effects of this phenomenon are only noticeable for a total antenna system gain of greater than 30 dB [6].

The more important effect of tropospheric turbulence is the resultant scatter—called "troposcatter"—when a small portion of the incident beam is deflected and creates a weak signal alongside the main beam. This signal may cause interference to an AIS receiver outside of the SOTDMA cell, or it may allow over-the-horizon transmission. In either case, this weak signal is the subject of an interference prediction.

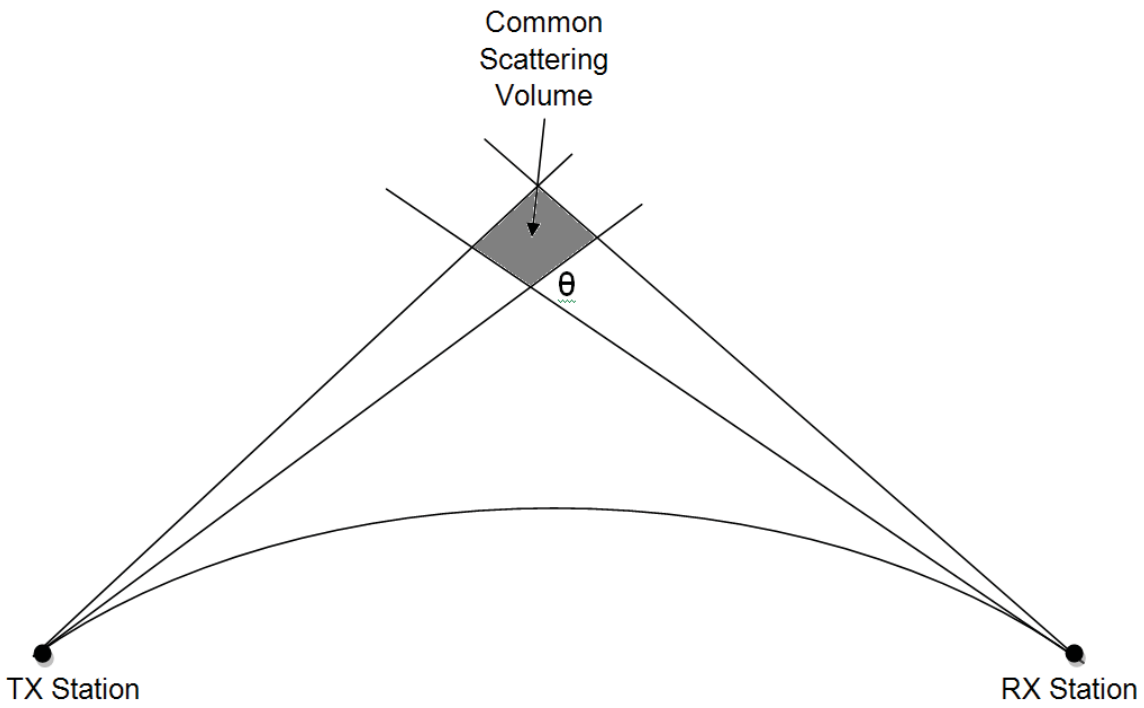

Figure 4: Geometry of tropospheric scattering

Tatarski [7] has outlined the underlying theory of radio wave propagation through the turbulent atmosphere. The model has been used to predict backscatter and forward scatter, but in the case of interference prediction in communication systems the theory is not deemed to be accurate enough [5]. Other theoretical models which deal with interference scenarios become very complex [2].

A simpler, semi-empirical model was therefore adopted by the ITU for the purposes of interference prediction. The model chosen for the ITU recommendation ITU-R P.452 was a derivative of the Yeh model. The basic transmission loss in decibels which is not to be exceeded *p* percent of the time is given as [2]:

$$L_{bs} = 190 + 30\log(f) + 20\log(d) + 0.573\theta - 0.15N_0 + L_c + A_g \\ -10.1(-\log(p/50))^{0.7} \tag{9}$$

where f is the frequency in megahertz, d is the distance in kilometres, θ is the scattering angle in degrees, and N_0 is the antenna gain correction factor.

A_g is the gaseous absorption factor calculated according to ITU-R P.676. It is based on a value of 3 grams per cubic metre because, while low, most of the troposcatter path is well above the earth's surface. Note that for the purposes of AIS frequencies, A_g < 0.005 dB per kilometre, according to the graphs in ITU-R P.676. N_0 is the surface refractivity which can be inferred from the map given in the text of the ITU-R recommendation P.452-14.

For a typical AIS setup, with operating frequencies of 160 MHz, a range of 120 km, and a resulting scattering angle of about 3.5°, the loss which is not to be exceeded 0.01 percent of the time is:

$$L_{bs} = 190 + 66.1 + 41.6 + 2 - 48 + 0.6 - 25.2 = 227.1\text{dB} \tag{10}$$

Hence this is the minimum loss for 99.99% of the time. For a 12.5W class A AIS transponder, this yields a received power of -216 dBW which is well below the typical AIS receiver sensitivity of -137 dBW. Hence troposcatter is deemed to be of small consequence in extending AIS transmission beyond the horizon.

Refractive Index of Air

The basic theory of refractive index can be found in many undergraduate texts. The refractive index is closely related to the relative permittivity of the medium, ε, being equal to its square root. Therefore the refractive index can be investigated by applying the methods of electromagnetism to atomic and molecular models. It is customary to begin by studying the relative permittivity in the static or dc (dielectric constant) case because this is simple. It turns out that the value of ε-1 for dry air is about 5.75×10^{-4} and varies by less than 1% over the frequency range from dc to 24 GHz, for example [8]. It is quite close to this value even at optical frequencies.

There are three mechanisms that result in the polarization of air [9]. The first applies to non-polar gases and is due to the distortion of the electron orbits about the nucleus in a small electric field. The distortion gives rise to a dipole moment, $\boldsymbol{p}$, for each molecule. This dipole moment is proportional to the field, $\boldsymbol{E}$, at the molecule; in the application to radio propagation the deviations from vacuum permittivity are very small and we can assume that $\boldsymbol{E}$ is just equal to the applied field:

$$\boldsymbol{p} = \alpha \boldsymbol{E} \tag{11}$$

where α is the polarizability of a molecule. It follows that the induced electric moment per unit volume, $\boldsymbol{P}$, is given by:

$$\boldsymbol{P} = n_0 \alpha \boldsymbol{E} \tag{12}$$

where n_0 is the number density of molecules. However, from considerations of electric displacement, we have:

$$\boldsymbol{D} = \boldsymbol{P} + \varepsilon_0 \boldsymbol{E} = \varepsilon \varepsilon_0 \boldsymbol{E} \tag{13}$$

where ε_0 is the permittivity of free space. Therefore:

$$\varepsilon - 1 = n_0 \alpha / \varepsilon_0 \tag{14}$$

When the left hand side is very small, this is identical to the Clausius-Mossotti equation, which applies more generally [8]:

$$\frac{\varepsilon - 1}{\varepsilon + 2} = \frac{n_0 \alpha}{3\varepsilon_0} \tag{15}$$

The atoms and molecules He, H_2, O_2, N_2 and CO_2 have zero dipole moments in the absence of an electric field so that (14) applies. However, (14) can be recast using the ideal gas law:

$$P_g V = n_g RT \tag{16}$$

where P_g is the pressure, V is the volume, n_g is the number of moles, R is the gas constant and T is the temperature. For unit volume we have:

$$n_g = n_0 / N_A \tag{17}$$

where N_A is Avogadro's number. Therefore (15) becomes:

$$\frac{\varepsilon - 1}{\varepsilon + 2} = \frac{\alpha P_g N_A}{3RT\varepsilon_0} = \frac{\alpha P_g}{3kT\varepsilon_0} \tag{18}$$

where k is Boltzmann's constant ($R = N_A k$) . It follows that for dry air, the difference between the relative permittivity and vacuum is approximately proportional to pressure and inversely proportional to absolute temperature.

Water, H_2O, is a polar molecule because the atoms form a triangle, unlike the previous molecules, which exhibit symmetry in their arrangement. This results in a permanent dipole moment, μ. Therefore, when water vapour is introduced into air, there is an additional contribution to the permittivity.

The water vapour molecules with their associated dipoles experience collisions with their neighbours and these tend to randomize their orientation. When a static electric field is applied, there will be a tendency for the dipoles to align with the field. This can be calculated according to statistical mechanics, and the electric moment per unit volume is given by:

$$\boldsymbol{P} = \frac{n_0 \mu^2 \boldsymbol{E}}{3kT} \tag{19}$$

Adding this contribution to that derived earlier we have for the static permittivity:

$$\frac{\varepsilon - 1}{\varepsilon + 2} = \frac{p_{Dry}}{3kT\varepsilon_0}\alpha_{Air} + \frac{e}{3kT\varepsilon_0}\left(\alpha_{H_2O} + \frac{\mu^2}{3kT}\right) \tag{20}$$

where p_{Dry} and e are the partial pressures of dry air and water vapour respectively.

In practice the permittivity can be modeled by introducing empirical constants, $K_{1,2,3}$ [10]:

$$\varepsilon - 1 = K_1 \frac{p_{Dry}}{T} + K_2 \frac{e}{T} + K_3 \frac{e}{T^2} \tag{21}$$

In radio propagation studies, it is convenient to work in term of the refractive index, *n*, rather than the permittivity. Because both the refractive index and the permittivity are close to one, we have:

$$1 - \varepsilon = (1 - n^2) \approx 2(1 - n) \tag{22}$$

According to [10], this yields the refractivity, *N*:

$$N = (n-1)10^6 = \frac{77.6}{T}\left(p + 4810.0 \frac{e}{T} \right) \tag{23}$$

where *T* is in degrees K and both *p* (the total atmospheric pressure) and *e* are in millibars. The coefficients are based on 0.03% of carbon dioxide and the equation of state for air rather than the ideal gas law. Smith and Weintraub [10] claim that this expression for the refractivity is accurate to 0.5 per cent for radio frequencies up to 30 GHz within the normal ranges of temperature, pressure and humidity. This equation has been used to model atmospheric refractivity for propagation studies [11]. There is a long history of measurements and the resolution of problems. In particular, no evidence of dispersion for frequencies up to 24 GHz was found by the authors of [12]. Much effort has been spent on estimating the refractive index accurately at optical frequencies, e.g. [13], [14] and [15]. Some of this could be relevant.

It is noted that the proportion of CO_2 in the atmosphere has increased to about 0.04% since Smith and Weitraub published their data. This suggests that some minor adjustments to their constants could be advantageous.

The polarization of a gas with polar molecules intimately involves collisions between the molecules. This is because the angular momentum of a molecule is quantized and an applied electric field of practical magnitude cannot excite a molecule out of its ground state. Therefore the orientation of the molecules cannot respond to the field unless a collision takes place. At low frequencies there are many collisions per cycle of the field and re-orientation under the field takes place many times. At angular radio frequencies, ω, of the order of the collision frequency, re-orientation of the molecule cannot occur smoothly and the polarizability will fall. As in the Debye theory of polarizability, the effect can be modeled as a viscous damping with a relaxation time, τ. This introduces a factor into the polar component of the induced dipole moment equal to:

$$\frac{1}{1 + i\omega\tau} = \frac{1 - i\omega}{1 + \omega^2\tau^2} \tag{24}$$

This has an imaginary part that represents the radio frequency energy absorbed by the collisions. Simplistic theory suggests that significant roll off in the real parts of the relative permittivity and refractivity could start at microwave frequencies of about 1 GHz but for water vapour this is not observed.

To render (23) useful, it is necessary to express the partial pressure of water vapour in terms of relative humidity, which is the quantity that is readily available in meteorological data. This can

be implemented using tables or estimated using the Clapeyron equation from thermodynamics. It relates the rate of change of saturated water vapour pressure, e_s, with temperature to the molar latent heat, L, and the molar volumes, V_v, of the vapour and the liquid, V_l, i..e.

$$\frac{de_s}{dT} = \frac{L}{T(V_v - V_l)} \tag{25}$$

For water $V_v >> V_l$ and applying the ideal gas law yields:

$$\frac{de_s}{dT} \approx \frac{e_s L}{RT^2} \tag{26}$$

On the assumption that L does not vary significantly with temperature, this can be integrated giving:

$$e_s = e_0 \exp\left(\frac{L}{R}\left(\frac{1}{T_0} - \frac{1}{T}\right)\right) \tag{27}$$

where e_0 is the saturated vapour pressure at T_0. For example, the actual water vapour pressure used in [11] is:

$$e = 6.11\, H\, \exp\left(19.7\frac{T-273}{T}\right) \tag{28}$$

where the units of e are millibars and H is the relative humidity as a fraction. This result is from [16] and it appears to be accurate to better than 1% over the temperature range 0 º to 45 º. Clearly T_0 is intended to be 0 ºC at which the saturated vapour pressure is 6.11 mbar (611 Pa). However, equating 0 ºC to 273 ºK rather than 273.16 ºK is not particularly accurate and could lead to small errors. A formula, due to Goff and Gatch is discussed in [17] but the values are not consistent with those of other workers. However, another useful formula for finding the vapour pressure is the Antoine equation [18]; for example the coefficients for a large number of organic liquids is given in [19].

For temperatures below freezing and down to at least -20 ºC, Ciddor [20] recommends the formula, which has a form that is similar to that above (as well as to the Antoine equation):

$$\log_{10} e_s = 12.537 - 2663.5/T \tag{29}$$

where e_s is now in units of Pa. Multiplying e_s by H gives the actual vapour pressure. It is easily verified that this gives the correct saturated vapour pressure at 0 ºC.

Fig. 1 shows the refractivity as a function of temperature and relative humidity at a pressure of 100 kPa and was calculated using (23) and (28). With high relative humidity, the refractivity rises with temperature because warm air can absorb more moisture.

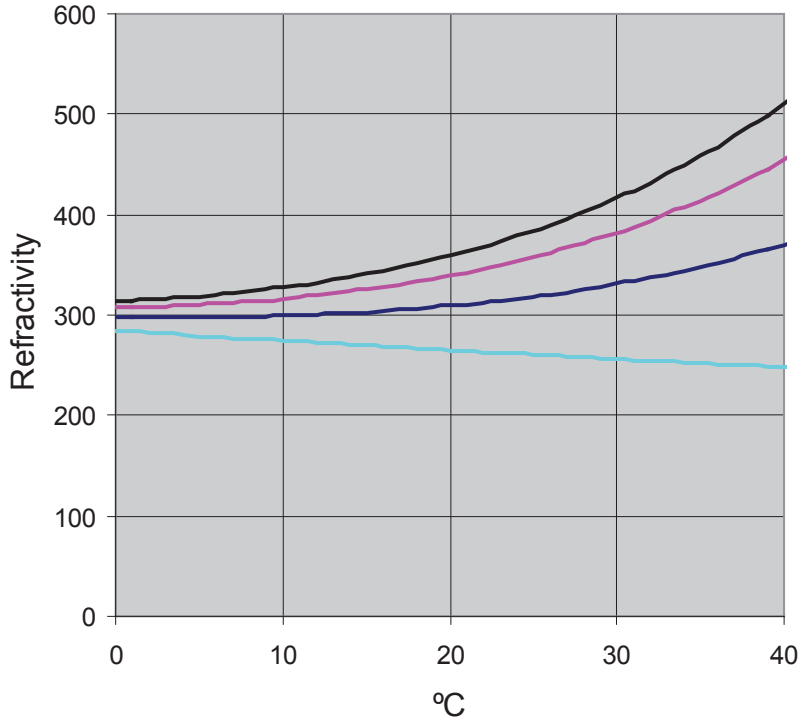

Figure 5: Refractivity of air as a function of temperature for relative humidities of 0% (—), 50% (—), 80% (—) and 100% (—).

Atmospheric Profile

The variation of the refractivity with height determines the propagation of VHF signals in air. This can be measured by a balloon-borne radiosonde. The preferred instrument is a microwave refractometer because this has a frequency response of tens of Hertz. This type of refractometer is based on the resonant frequency of a cavity, which depends on the dielectric constant of the air. Otherwise the pressure, temperature and humidity can be measured and the refractivity calculated using (23).

The profiles are discussed by Hall [16] and Barclay [2]. In temperate regions under normal atmospheric conditions the temperature decreases with height at a rate of about 6.5º/km and the pressure decreases approximately exponentially. This leads to a refractivity that decreases with altitude at a rate of about 40 km^{-1}. Signals are refracted slightly downwards and tend to follow the curvature of the earth. This raises the effective radius of the earth by a factor of approximately 4/3. For lower refractivity decreases, the signals will be refracted away from the "4/3 earth" and this is called "sub-refraction". For greater decreases, the range of the signals is extended and this is called "super-refraction".

Under conditions of temperature inversion, the refractivity decreases at a rate of more than about 157 km^{-1} and ducting can occur. This leads to propagation of VHF signals over very long

distances because the signals remain trapped within the duct and fall off with distance much less rapidly. Temperature inversion is a situation where the temperature increases with altitude rather than decreases. It can occur when

- Warm dry air lies over a cool surface, such as the sea;
- The land surface cools under clear skies;
- A warm front forces warm air over a cold surface; this is often associated with an anticyclone (high pressure);
- Sea breezes undercut warm air over land; and
- Cold downdraughts are associated with cumulonimbus clouds as may occur when there are heavy showers or thunderstorms.

It should be noted that a relationship involving the wavelength and the layer thickness must also be satisfied for ducting to occur. The ducts can extend up to 3 km in altitude.

Batianeh and Macario [11] describe a refractivity model in which an isothermal atmosphere is assumed so that the pressure profile is given by:

$$p = p_0 \exp\left(-\frac{gh}{RT}\right) \tag{30}$$

where p_0 is the pressure at the sea surface, g is the acceleration due to gravity, h is the height and T is the average temperature in the lower troposphere. In their model the temperature normally decreases linearly with height and the combined effect of the pressure and temperature variation is that the refractivity also decreases. Under conditions of temperature inversion, the temperature first increases with height from the surface and then decreases. The humidity also decreases with height and this causes the refractivity to fall with height; the refractivity lapse rate is high and refraction may be increased to an extent where ducting occurs. Details of the model can be found in the paper.

Refraction

In the simplest model, the refractive index of the atmosphere can be described by concentric spherical surfaces of constant index centered on the earth. The phase of an electromagnetic wave passing through one of the surfaces must be continuous through it. If the phase of the wave at the surface of constant refractive index is ϕ:

$$\phi = \omega t - \mathbf{k} \cdot \mathbf{r} \tag{31}$$

where ω is the angular frequency, t is the time, $\mathbf{k}$ is the angular wavevector and $\mathbf{r}$ the position vector along the surface. Therefore the refraction through the surface is described by $\mathbf{k} \cdot \mathbf{r}$ = constant. Because the frequency of the wave is a constant and the velocity of light in the medium is inversely proportional to the refractive index, $\mathbf{k}$ is proportional to n. The basic equation is Snell's law:

$$n\hat{\mathbf{k}} \cdot \hat{\mathbf{r}} = const \tag{32}$$

where the "hat" indicates a unit vector. In polar coordinates (r, θ), this becomes:

$$n\hat{\mathbf{k}}_{\mathbf{r}} \cdot \hat{\mathbf{r}} + nr\hat{\mathbf{k}}_{\boldsymbol{\theta}} \cdot \hat{\boldsymbol{\theta}} = const \tag{33}$$

However, the first term is zero because the surfaces of constant index are perpendicular to the radial direction. Thus we have [16] the polar coordinate form of Snell's law:

$$nr\cos\alpha = const \tag{34}$$

where α is the angle of the wavevector to the earth's surface. When the refractive index is a function of height, h, differentiation with respect to r yields:

$$\frac{1}{r} = -\frac{1}{n}\frac{dn}{dh}\cos\alpha \tag{35}$$

If we set $\alpha = 0$, and the radial coordinate, r, to the earth radius, we can find a refractivity lapse rate that just causes the ray to follow the surface of the earth; it corresponds to about 157 km^{-1} as already noted and corresponds to ducting.

Software

Some useful information on atmospheric and tropospheric effects at long range is provided in [21]. The formulae for finding the propagation losses under simple atmospheric conditions are provided. This is accompanied by a spreadsheet [22] from which the propagation loss under the refractivity (profile constant over the path) conditions can be estimated[8]. The spreadsheet estimates the propagation loss statistics for interference signals over land and sea paths. However, the calculations are the same if the "interfering signal" is simply an AIS signal.

AIS receiver characteristics are defined in [1]. This document states that the minimum receiver sensitivity for a 20% Packet Error Rate (PER) is -107 dBm or -137 dBW. This takes into account the thermal and other noise associated with bandwidth of the receiver to achieve the stated PER. The signal power, P_r, received from a transmitter over a free space path is given by:

$$P_r = \frac{P_t G_t G_r \lambda^2}{(4\pi r)^2 L_h} \tag{36}$$

where P_t is the transmitted power, G_t is the transmitter antenna gain, G_r is the receiver antenna gain, λ is the wavelength, r is now the path length and L_h represents other losses in the hardware. In this case the path loss, L, is given by:

$$L = \frac{\lambda^2}{(4\pi r)^2} \tag{37}$$

[8] Though saved as an "xls" file, the spreadsheet is designed to function using Excel 2007 and has been tested. There seemed to be problems running under Excel 2003. If the antenna heights are set very high and other parameters adjusted appropriately, the program calculates the correct free space propagation loss.

The spreadsheet provides the path loss in more general circumstances that include refraction due to variations in the atmospheric refractivity and diffraction at the earth's surface. As an example, consider the data in Table 6 for an ocean area off Vancouver Island

Table 6: AIS Parameters

Parameter	Value
Transmitter Power (dBW)	11.0
Transmitter Antenna Gain (dBi)	2
Receiver Antenna Gain (dBi)	2
Wavelength (m)	1.86
Path length (km)	120
Average Refractivity Lapse Rate (km^{-1})	44*
Maximum Monthly Mean Refractivity Lapse Rate(km^{-1})	55*
Sea Level surface Refractivity	325*
Height of Transmitting Antenna (m)	15
Height of Coastal Receiving Antenna (m)	50
Cable and Other Losses (dB)	3
Percent of Time that Signal Exceeds Calculated Value (%)	10
**From the data in the spreadsheet for Vancouver.*	

Now entering this data with appropriate latitude and longitude, the spreadsheet gives a propagation loss of 148.9 dB. The loss will be less than this for 10% of the time. Therefore the received power will be greater than 11 + 2 + 2 – 3 – 149 = -137 dBW for 10% of the time. Alternatively the result can be interpreted that the range will be greater than 120 km for 10% of the time. To establish a match to the AIS specifications generally requires some manual iteration in the range or other parameters.

Ray Methods

The simplest approach to predicting the propagation characteristics of radio waves is to employ ray theory. This is based on the geometric optics model. In free space the waves propagate in straight lines within ray tubes. The ray tubes vary in cross-section so as to be consistent with the conservation of energy. Ray models are scalar models and cannot properly represent polarization effects though the electric or magnetic vectors of the electromagnetic wave can point in a fixed direction with respect to the ray. However, the theory can be extended to accommodate scattering and polarization changes at discrete points along the ray. Based on geometric optics, ray models cannot easily encompass leakage of waves from the top of a layer or scattering from a rough ocean surface.

A principal effect of the troposphere is to bend the rays in an arc. If this follows the earth's surface, the ray will appear to propagate parallel to the surface. Therefore a simple coordinate transformation is often used which renders the earth flat. This corresponds to a refractivity gradient of close to -157 km^{-1}. If the refractivity is less than this, the rays in this coordinate system are curved upwards. If it is more than this, the rays are bent downwards and are reflected from the earth's surface; they tend to be confined in a duct. The model is known as the "flat earth model".

In the flat earth model the effect of the coordinate transformation is to change the refractivity from N to a new value M by adding 157 km $^{-1}$, which is an effective refractivity value for this model.

Applications to AIS must take into consideration that the transmitter and receiver will always be located close to the earth. This implies that elevated ducts should not be important. This simplifies propagation treatments because the height of a ray above the earth's surface will be confined within narrow limits where the flat earth approximation is valid; no elevation angle corrections are needed.

When the vertical gradient of the refractivity profile is less than that needed for ducting, the rays from a transmitter can be calculated in a trivial manner (especially when the profile is constant along the surface of the earth) and the receiver will either lie on a ray path or not. The amplitude of the received wave can be found by computing rays along a ray tube that passes through the receiver. If ducting occurs, the rays will be refracted and bounce within the duct; they can be computed in the same way though with a little more difficulty.

However, when the receiver is not directly in the path of a ray, such as when it is over the radio horizon, ray methods are not useful because, at least in their simple form, they ignore diffraction and the result is binary. A situation where the signal is simply received or not is not realistic. Therefore, while ray methods can be useful when there is ducting or when there are variations in the vertical refractivity profile along the surface of the earth, the parabolic equation method is preferred.

Ducting

A typical duct is of thickness, t = 25 m with a change of δN = 10 N-units, this represents a gradient of 400 km^{-1}. There is a wavelength cut-off [16] given by:

$$\lambda_{\max} = 0.0025\left(\frac{\delta N}{t} - 0.157\right)^{1/2} t^{3/2} \tag{38}$$

For this example, the cut-off is 0.15 m, which is far less than the AIS wavelength of about 2 m. Therefore the AIS signals will not be able to propagate in such a duct. According to (38), the thickness of the duct would have to be about 150 m with a change in refractivity of 50 N-units. This would occur less frequently.

Rays can only enter a duct in a limited range of angles. This reduces the power that can be transmitted over long distances. Rays propagating at angles greater than a critical angle, θ_c, will leave the top of the duct and those that start below a critical angle will hit the ground. Hall states that:

$$\theta_c = \sqrt{2\Delta M \times 10^{-6}} \tag{39}$$

Rays are trapped between $\pm\theta_c$, where the units are radians [16] and ΔM is the decrease in effective refractivity between the transmitter height and the top of the duct. According to Hall, the critical angle never exceeds 0.5 degrees.

The additional path attenuation (over and above the free space loss) associated with a duct can be positive or negative and according to Hall is given by:

$$C_1 d - 10 \log d + L_c \tag{40}$$

where d is the path length (in kilometres) within the duct. At AIS wavelengths, the constant C_1 is approximately 0.1 dB/km. The second term is negative because the power falls off more slowly than in free space. For the present purposes, the last term [16] is given by:

$$10 \log(2\theta_c / \theta_B) \tag{41}$$

Here θ_B is the half power antenna beam width. In the case of an AIS system, where the antennas are almost isotropic the antenna beam width nominally approaches π radians. However, estimates in terms of solid angles would be an improvement.

Ducts are produced by evaporation and advection. Tropical heating produces a humid layer over the sea with a drier layer above. This is prevalent in the afternoon with a typical thickness of 15 m. Ducts may be an almost permanent feature of tropical seas. They can also form when hot dry air from land blows over the sea in the evening; the typical thickness is 25 m. Other mechanisms are described in [16].

Parabolic Equation Methods

The parabolic equation method is described in [2]; in [23] it is treated in detail. The method can be applied to propagation through the troposphere over sea and land. It is usually applied to two-dimensional problems so that the model for the signal is based on a scalar wave equation so that polarization is either horizontal or vertical. Further simplification is achieved by assuming that the waves propagate close to some preferred direction. In other words the problem involves paraxial waves. Also the tropospheric variations in refractivity are usually handled in such a way as to effectively flatten the earth.

The advantage of the parabolic method is that Fast Fourier transform or finite difference techniques can be employed to render solutions by a marching technique in which solutions are found at increasing range. For applications to propagation over the sea, the method can be implemented on a desktop computer in seconds. The model can include scattering off the rough surface of the sea and the leakage of waves from a tropospheric duct.

Details of the theory and applications are described by Levy [23]; the steps are as follows:

1. Reduce Maxwell's equations to a second order Helmholtz equation with a refractive index as a function of range and height.
2. Assume an oscillatory variation in the range direction.
3. Assume paraxial propagation in the range direction.
4. Factor the resulting equation into first order forward and backward propagating terms.
5. Approximate a square root operator, often by a simple power series.
6. Approximate propagation by the split-step Fourier method or the finite difference method.

Levy explains that the first three steps allow the second order differential equation arising from the scalar approximation to Maxwell's equations (the Helmholtz equation) to be factored into two parts: namely forward and backward waves. While it may be legitimate to ignore the backward wave in some applications, such as propagation over the sea, this is not true generally. Therefore a pair of first order coupled equations must be solved.

When backward waves and edge currents are neglected, Levy shows that the parabolic method applied to a semi-infinite screen in a vacuum reduces to the standard Fresnel diffraction result.

The split-step method handles propagation by separating the medium in the range direction into vacuum segments separated by phase screens. The vacuum regions are sufficiently thin that the refractive index does not vary significantly with range over the width of the segment. Boundary conditions at the top and bottom of the segment must be satisfied. For example, when the sea is smooth and an earth flattening approach is used, the boundary condition over the sea is that the field is zero at the bottom of each segment. At the top of a segment the waves must be outgoing only.

The treatment of propagation over a rough sea is only important when there is at least one reflection off the sea surface. This will be true for any trans-horizon path. Reflection depends on the relative magnitudes of the root mean square sea height and the wavelength. This can be expressed in terms of a Rayleigh roughness parameter, γ given by:

$$\gamma = 4\pi\sigma \sin\alpha / \lambda \tag{42}$$

where σ is the rms sea height, α is the grazing angle and λ is the wavelength; the rms sea height can be expressed entirely in terms of the wind speed. If this is small, perturbation techniques are valid. However, the wavelength of AIS signals is about 2 m, which is of the same order as sea height variations in high sea states. Therefore a roughness reduction factor, ρ, can be introduced to account for the reduction of the reflection coefficient for a flat surface:

$$\rho = \exp\left(-\frac{\gamma^2}{2}\right) I_0\left(\frac{\gamma^2}{2}\right) \tag{43}$$

where I_0 is a modified Bessel function.

The parabolic equation method requires the surface impedance for its lower boundary condition. The surface impedance, δ, for a plane wave can be expressed in terms of the reflection coefficient, R, which is modified by the reduction factor (as outlined by Levy, p 170):

$$\delta = \sin\alpha \frac{1-R}{1+R} \tag{44}$$

Hybrid models, which combine geometric optics solutions over high altitude paths and parabolic methods, are discussed by Levy but, for the purposes of analyzing AIS signals, the parabolic method is probably the most suitable. Criteria are provided to indicate an appropriate solution domain.

An example of the use of parabolic methods for propagation over a sea surface is provided in [24]. This was based on a parabolic method with a forward wide angle propagator. A comparison was made between measurements at 818 MHz and simulations. The authors claim that excellent agreement was obtained in one case but in the other the ducting conditions were not properly met and agreement was not as good.

Lightning

The literature on the effects of lightning reflections is very limited. There has been anecdotal evidence (found on certain web resources such as [25]) that scattering can occur which result in ranges of up to 700 miles. The ionization that occurs during a lightning strike results in a scattering mechanism similar to that of meteor trails (see section 5.3). The strike must occur roughly halfway between the transmitting and receiving station, as well as during the length of the transmission, in order for interference to result. Hence it is deemed that this interference mechanism will have adverse AIS effects which are unlikely to occur.

Hydrometeors

When water condenses in the atmosphere, it can take on a variety of forms: rain, fog, clouds, snow, and hail. Collectively these are known as hydrometeors. Their effect on radio wave propagation is dependent on both the system frequency and the size and type of particle that the wave encounters. [2]

Of the mentioned hydrometeors, rain is the most important in the VHF band [6]. The rain drop size distribution is central to theoretical analysis. The distribution function is denoted $N(D)dD$, which represents the number of drops with diameters between D and $D + dD$ per cubic metre. The model most commonly chosen is an exponential form:

$$N(D) = N_0 \exp(-\Lambda D) \tag{45}$$

Where lambda is related to the rainfall rate R in millimetres per hour via:

$$\Lambda = 4.1R^{-0.21} \tag{46}$$

The rainfall rate is also related to the integration of the drop size distribution function [6]:

$$R = 0.6 \times 10^{-3} \int_D D^3 V(D) N(D) dD \tag{47}$$

Where $V(D)$ is the terminal velocity of a drop of size D in metres per second. The Marshall-Palmer distribution yields a typical value for N_0 of around 8000 mm per cubic metre [6]. Various other forms of the rain drop size distribution function have been proposed. None are regarded as been consistent with physical reality, but all are considered accurate enough for modeling.

The far field scatter is determined by a scattering function $S(\theta)$. For the purposes of forward scatter, $S(0)$ is the parameter of interest. In the Rayleigh scattering region ($\pi D << \lambda$), then [2]:

$$S(0) = jP\omega^3\mu_0 / 4\pi c \tag{48}$$

where $\omega = 2\pi f$ is the radial frequency of the impinging electromagnetic wave, μ_0 is the permeability of free space, and c is speed of light in a vacuum. The induced dipole moment, P, for a spherical water drop is:

$$P = 3z\varepsilon_0 v \tag{49}$$

where $z = (\varepsilon_r - 1)/(\varepsilon_r + 2)$ is a complex value based on the relative permittivity of water, and v is the volume of the particle. Also of interest is the total extinction cross section of a particle, C_{ext}, which is the portion of incident energy that is absorbed and scattered. C_{ext} is given as

$$C_{ext} = \frac{\lambda^2}{\pi}\mathrm{Re}[S(0)] \tag{50}$$

Combining these three equations, the expression for the total extinction cross section becomes:

$$C_{ext} = \frac{\pi^2 D^3}{4\lambda}\mathrm{Im}[z] \tag{51}$$

Finally, the total attenuation for a path of length L can be found from [2]:

$$A = 4.34L\int_0^\infty C_{ext}N(d)dD \tag{52}$$

Evaluation of this integral for a rainfall of 10 millimetres per hour at a typical AIS frequency of 160 MHz (and a corresponding value of approximately 0.0001 for Im[z] as extrapolated from the graph in [2]) yields an attenuation of approximately 0.000018 dB per kilometre, which is negligible for a typical signal path length on the order of hundreds of kilometres.

Interference from backscattering of a radio wave in a common scattering volume is possible. To find the power received from the backscatter, the radar cross section of a single drop is found to be [6]

$$\sigma_d = \frac{\lambda^2}{\pi}\left(\frac{\pi D}{\lambda}\right)^6 |z|^2 = \frac{\pi^5}{\lambda^4}|z|^2 D^6 \tag{53}$$

For convenience, a parameter known as the atmospheric reflectivity factor is introduced

$$Z = ND^6 \tag{54}$$

where N is the number of particles per unit volume so that Z has units of mm^6/mm^3, and hence a multiplying coefficient of 10^{-18}. The cross section per volume is then given as:

$$\sigma_D = \frac{\pi^5}{\lambda^4}|z|^2 Z \tag{55}$$

Z has been related to the rainfall rate R by this relation from the ITU:

$$Z = 400R^{1.4} \tag{56}$$

Hence the ratio of received power to transmitted power becomes:

$$\frac{P_r}{P_t} = \frac{G_t G_r \lambda^2 V \sigma_D}{64\pi^3 R_t^{\,2} R_r^{\,2}} = \frac{G_t G_r \pi^2 V Z |z|^2}{64\lambda^2 R_t^{\,2} R_r^{\,2}} \tag{57}$$

where V is the common scattering volume between the receiving antenna at a distance of R_r, and transmitting antenna at a distance of R_t. For frequencies up to 100 GHz, $|z|^2 = 0.93$ to a very good approximation [6].

Note that this expression assumes a constant rainfall throughout the entire common scattering volume. A more accurate representation results when an integration of constituent radar reflectivities is taken over the entire scattering volume. This is further outlined in ITU-R P.452-14 [26].

It can be inferred from the above equation that the received power decreases with square of increasing wavelength. Barclay summarizes an experiment conducted at 11.2 GHz between Baldock and Chilbolton in the UK – a range of about 131 km. The transmission loss does not exceed 130 dB for 0.001 percent of the time [2]. A typical AIS frequency of 160 MHz has a wavelength which is 72 times greater than at 11.2 GHz. Hence the further transmission loss for AIS frequencies would be $20\log(72)$ = 37 dB more than at 11.2 GHz, or approximately 167 dB. For a 12.5 W class A AIS transponder and isotropic antennas, this corresponds to a received power of -156 dBW which is below the typical AIS receiver sensitivity of -137 dBW.

Ionosphere Effects on AIS Technology

The ionosphere is a portion of the upper atmosphere which has adequate ionization to affect the propagation of VHF signals. Two regions of the ionosphere—the D region and the sporadic E region—are most likely to cause scattering and reflections. Meteors entering the ionosphere also produce ionized trails which can reflect VHF energy. These effects and their impact on VHF propagation are evaluated in the context of AIS transmission.

D Region

The D Region of the ionosphere extends from 50 to 90 km above sea level and is produced by Lyman α and X-rays. Scatter in the D Region can occur at heights of 70 to 90 kilometres. Upper troposhere turbulence can cause fluctuations in the electron density of this region, which in turn can lead to the scattering of RF energy [27]. Usually the scatter occurs at small angles to the incident beam, and hence is called "forward scatter." Bailey et al. [28] give the ratio of power received (P_r) to power transmitted (P_t) in the general form:

$$\frac{P_r}{P_t} = \frac{f_p^{\,4}}{f^m} \frac{A(\sin(\chi/2))^2}{l^2(\sin(\gamma/2))^n} \tag{58}$$

Where A is the total gain of the antenna system, f is the operating frequency, l is the ray path length from the transmitter to the ionosphere layer in question, γ is the scattering angle, and χ is the angle between the incident electric vector and the direction of the scattered wave. The plasma frequency f_p is defined in (61) in section 5.3. It is found that for high and mid latitudes, the value of m can vary with time between 7 and 9.5. The value of n can vary between 4 and 12 depending on the season. It should be noted that the received scattered power decays as an inverse to the square of the path length, since the scattering volume increases for an increase in range.

Davies [27] summarizes the long term variations of the received signal strengths presented by Bailey et al [28]. It was found that for signals between 25 MHz and 108 MHz, and for distances between 1000 and 2000 km, the recorded system losses between transmitter and receiver were between 140 dB and 210 dB. As the above equation states, the received power decreases sharply for an increase in frequency.

For the purposes of AIS interference, a particular setup outlined in Bailey et al. [28] is considered. In it, the path length is 1251 km, the system frequency is 107.8 MHz, and a system loss of 115 dB is measured relative to the free space path. The loss is then extrapolated based on (58). A value of $m = 7$ is chosen for the frequency dependent factor, since it would provide the least amount of further path loss. Adjusting for a typical AIS frequency of 160 MHz, and adding the inverse distance loss for a path length of 300 km yields a further path loss of:

$$70\log(160/108) + 20\log(300) = 61\text{dB} \tag{59}$$

Thus received signals from a 12.5W Class A AIS transponder would have a power level of 11 - 115 – 61 = -165 dBW which is much less than the specified AIS receiver sensitivity of -137

dBW. It is hence unlikely that scattered AIS signals from the D region would arrive at a high enough power to effectively extend the transmission range.

Sporadic E

The sporadic E region (E_s) of the ionosphere is comprised of thin layers (often less than 1 km) of enhanced ionization 100-120 kilometres above sea level. These layers vary greatly by season, geographical location, and time of day – hence sporadic. These layers are dense enough to affect radio wave propagation. In general, there are three types of sporadic E layers [2]:

1) Mid Latitude: caused by wind shears and possibly meteors interacting with the geomagnetic field;
2) Equatorial: instabilities are caused by large electron drift velocities from the electrojet; and
3) Auroral: produced by the precipitation of kilovolt electrons;

The effects of propagation within the sporadic E layer have been deemed to be negligible at frequencies greater than 90 MHz, except as a potential interference source [27]. Further, it has been well documented that the impact of these sporadic E effects decrease with increasing frequency. Hence most of the literature has examined the statistical impact of sporadic E effects at frequencies much lower than the ~160 MHz which an AIS system employs.

For a vertically incident signal to be reflected back to earth, there must be adequate ionization in a particular sporadic E cloud to support a critical frequency fE_s. Any frequencies above fE_s will pass through the sporadic E layer. A signal obliquely approaching the cloud is found to have a lower equivalent vertically incident frequency by dividing the incident frequency by the secant factor arising from the geometry of the transmitter-receiver setup [2].

Davis et al. [29] examined the sporadic E effect on VHF propagation from Cedar Point to Sterling over a period of four years. The frequencies selected were 27.775 MHz and 49.8 MHz. Plotted are the probabilities that a given received signal intensity will exceed the ordinate. These probabilities are of approximately an order of magnitude lower at 49.8 MHz (between 0.01% and 1% of the time) versus at 27.775 MHz (between 0.1% and 10% of the time).

This is in accordance with the Philips rule, also known as the frequency dependence rule, which states the probability of fE_s being greater than the signal frequency f – and hence permitting reflection of the signal back to earth—is related to the signal frequency f (in MHz) by the following [26]

$$\log(p(fE_s > f)) = a + bf \tag{60}$$

Where the parameters a and b are empirically determined. Dazhang et al. [30] have calculated values for these parameters for 18 different sites in China. It was found that the frequency dependent coefficient b had values between -0.1683 and -0.4943, with an average of approximately -0.2, confirming the rapid drop-off of probability of fE_s reflection with increased signal frequency. Substitution of a typical AIS frequency of ~160 MHz into the geometry of the Cedar Point to Sterling setup would yield a likelihood of sporadic E interference approximately

40,000 times less likely than at 49.8 MHz. Hence sporadic E reflections are insignificant when considering AIS signals.

Meteor Trails

A consideration of the scattering of signals at AIS frequencies by meteor trails is important because in principle it can lead to interference from AIS transmissions outside of the SOTDMA cell as well as from land-based radio transmissions. The range can be over 200 km and interference via a single meteor trail might occur for a second or two.

Meteor scattering has been reviewed by Davies [27]. The most important meteors for radio propagation are sporadic meteors, which arrive randomly in time and from random points on the celestial sphere. In contrast, shower meteors tend to arrive at specific times when the earth crosses the orbital path of a debris stream. Shower meteors often seem to radiate from specific constellations, for which they are named. Davies states that reflections are observed at frequencies in the range 30-110 MHz, which is somewhat less than the AIS frequency of about 160 MHz. Therefore, at the outset a serious problem is not expected.

A meteor trail can be regarded as a reflecting cylinder of ionized air at altitudes from about 80 km up to 120 km with a length of up to 50 km and a diameter of several metres. The trail is characterized by the density of free electrons per unit length and this density increases with the original mass of the meteor. The frequency of occurrence of a meteor decreases rapidly with mass so that meteors with a mass greater than 1 gram intersect the earth about 10^5 times per day and produce a line density of more than 10^{17} electrons/m.

An ionized trail in the upper atmosphere spreads in radius due to diffusion. The initial radius is of the order of 1 m and expands to tens of metres in a few seconds, depending on the height. If the radio frequency is less than the plasma frequency, the trail scatters like a conducting metallic cylinder because the radio wave cannot penetrate it. This is known as an "over-dense" trail. As the trail expands the scattering increases until the plasma frequency, which is proportional to the electron number density, falls below the radio frequency and the radio waves penetrate the trail. In this latter case, the scattering can be described in terms of individual electron scattering and the trail known as "under-dense". The scattered amplitude is now reduced because of interference effects in the radial direction over the entire cross-section. The wavelength of AIS signals is about 1.9 m so that interference will be important for under-dense trails of radius greater than 1 m.

The incident and reflected rays make equal angles to a normal to the cylinder and all three vectors must lie in the same plane. Thus geometrical conditions must be met if bistatic communication is to take place. However, these conditions will be met frequently.

The plasma frequency f_P depends on the electron density, n_e:

$$f_P^2 = \frac{n_e e^2}{4\pi^2 m \varepsilon_0} \tag{61}$$

where e and m are the charge (1.6×10^{-19} C) and mass (9.1×10^{-31} kg) of an electron and ε_0 is the permittivity (8.85×10^{-12} F/m) of free space. Solving this for the electron density using the AIS frequency of about 160 MHz yields $n_e = 3.2\times10^{14}$ m^{-3}.

Davies provides a table of meteor frequencies and electron line densities. The electron density just calculated with an initial trail radius of a few metres corresponds to meteors of mass 10^{-2} g that intercept the earth about 10^7 times per day. However, most of the trails will not be visible to an AIS receiver and the number in a radius of about 200 km is about 2500 per day.

For the purpose of estimating the signal strength of an AIS transmission, the trail can be considered as an over-dense, perfectly conducting reflector with radius 5 m located at a distance of 100 km from both the AIS transponder and the terrestrial ground station. Apart from a geometrical factor, which must be applied for bistatic communication and which is of the order of unity, the effective length of the trail, L, is equal to one half of the Fresnel zone size, i.e.:

$$L \approx \left(\frac{R\lambda}{2}\right)^{1/2} \tag{62}$$

where R is the distance of the reflection point to the receiver (and transmitter in this case) and λ is the AIS wavelength. Therefore, applying the geometrical optics approximation [31], the RCS, σ, is given by:

$$\sigma \approx \frac{2\pi aL^2}{\lambda} = \pi aR \tag{63}$$

where a is the trail radius. (The definition of RCS is not the same as that in [27] but is consistent with that normally used in radar work such as [32] and [31]; Davies' version is less by a factor of 4π.) For a = 5 m, this gives a practical upper limit to the RCS of about 1.5×10^6 m^2.

In mobile applications we can assume that the antennas are approximately omni-directional though some small gain can be achieved by restricting the antenna pattern in the vertical direction. Therefore the received power, P_r, is related to the transmitted power by (e.g. [27] and see remark above):

$$P_r = \frac{G_r G_t P_t \lambda^2 \sigma}{64\pi^3 R^4} = \frac{G_r G_t P_t \lambda^2 a}{64\pi^2 R^3} \tag{64}$$

Assuming isotropic antennas ($G_{r,t}$ = 1), the received power from a 12.5 W Class A AIS transponder is about -155 dBW. This must be compared with the specified AIS receiver sensitivity of -137 dBW; the signal is 18 dB smaller than the receiver sensitivity.

Therefore under normal circumstances reflections of AIS signals from meteor trails can be ignored unless the meteor is very large. This is quite rare (see Davies [27]). Also the AIS transmission has to occur within the time (one or two seconds) that the meteor trail exists. However, in high shipping densities, the rate of transmission of AIS signals into a single TDMA slot could approach or even exceed one hundred per second. Then meteor scatter would provide a seriously noisy background for a significant fraction of the time.

Interfering land-based transmissions could be a problem if the transmitter power is of the order of 1 kW or more but this is unlikely because the internationally agreed spectrum allocations do not permit these signals in the AIS band.

Other Propagation Effects

Other effects which are not native to the troposphere or the ionosphere can also impact VHF propagation. VHF energy can arrive at a receiver via more than one path either constructively or destructively adding, an effect called multipath. As a signal propagates over land, various obstacles along the path can cause diffraction and attenuation. The signal can also be diffracted over a smooth surface such as the sea, allowing it to follow along the curvature of the earth. These various propagation effects are considered in the context of AIS signal transmission and their respective impacts evaluated.

Multipath

The signal strength at the receiver is proportional to the transmitted power. For AIS Class A signals the power in the ITU specification is 12.5 W. However, in practice it may be substantially less than this because the transmitter is degraded and the cabling and antenna are corroded by salt water. Therefore some care must be exercised in interpreting observed signal strengths.

When a signal arrives over several different paths, the average power is additive, which is a positive effect. On the other hand there is the possibility of cancellation, which may be sufficiently severe to cause message corruption or signal loss. It should be noted that AIS is designed as a collision avoidance system and that signals are transmitted from a ship under way at intervals of seconds. Therefore AIS will function for the purpose of collision avoidance even with a greatly reduced transmitted power as well as severe multi-path effects. This is not helpful when the objective is reliable reception at long range.

Multi-path causes three effects. These are variations in signal strength at the receiver, changes in phase that may be sufficiently rapid to affect carrier recovery in a coherent receiver and a spread in the information carried by the signal in time (group delays). It is a result of the signal propagating over different paths of different length so that the received complex amplitude is the sum of two or more contributions. These can combine in different ways in the complex plane so as to augment the received amplitude or reduce it to the extent that a signal may fade out entirely.

For AIS, there will typically be propagation paths involving rays reflecting from different parts of the transmitting ship superstructure as well as from the ocean surface. An AIS antenna may take the form of a vertical whip and ideally this would be mounted above and away from other parts of the ship. Unfortunately this is often not the case and the signal may be obscured and, in some directions, may be diffracted around obstructions. Overall this leads to signal losses and multi-path propagation.

Consider a receiver that is ship based or shore based. In both cases reflections can occur that contribute to multi-path. In the case of a shore based receiver, efforts are generally made to ensure that the antenna is not obscured and that multi-path propagation is minimized. However, reflections from the sea surface at low angles of depression may be difficult to avoid and reflections from the terrain are possible.

At grazing incidence, a surface such as the sea may have significant roughness but can act as if it were smooth to the radio waves. Therefore it can act like a highly reflective mirror with only a small fraction of the energy being scattered randomly and most being reflected specularly [2]. This is discussed at length by Hall [16], Chapter 4. It is stated that roughness with a standard deviation in height of σ_0 introduces a factor, k, reduction in the specular component of the reflected amplitude given by:

$$k = \exp\left(-\frac{1}{2}\left[\frac{4\pi\sigma_0 \sin\alpha}{\lambda} \right]^2 \right) \tag{65}$$

where α is the grazing angle and λ is the electromagnetic wavelength. The scattered or diffuse amplitude component tends to be Rayleigh distributed and its phase is incoherent.

Multi-path propagation can be based on a model in which each path contributes signal amplitude that can be regarded as a vector in the complex plane. Signals from different paths contribute vectors with arbitrary phase. Moreover, as the ship and sea moves, the phase is apt to vary in time. Therefore the model is one in which random vectors change their orientation. This suggests that, at any instant of time and if the number of paths is large, the complex amplitude is approximately normally distributed ("Gaussian") and the phase is uniformly distributed over the interval [0, 2π]. The phase variations are described in terms of a characteristic or correlation time.

The theory is provided in [4] and [33]. When the complex amplitude is normally distributed, the signal amplitude is Rayleigh distributed and the signal power is exponentially distributed (the exponential distribution is identical to the chi-squared distribution with two degrees of freedom). When the direct signal path dominates the received signals and other paths are relatively small and randomly phased, the received signal is better represented by a constant vector with noise added; a more appropriate distribution is the Ricean distribution. In other cases the Nakagami-m distribution is a better fit to data. The Nakagami-m distribution is related to the gamma distribution in probability theory [34]. It is a one-sided distribution and the parameters are the mean and a shape parameter. This distribution appears not to be grounded in theory but is based purely on the fact that it can be made to fit data. For heavy fading, the log-normal distribution may be used.

Expressions for the distributions are given in [33]. The Rayleigh density is given by:

$$p(x) = \frac{x}{\sigma^2} \exp\left(-\frac{x^2}{2\sigma^2} \right) \tag{66}$$

where σ^2 is the variance related to the mean, μ, by $\mu = 1.253\ \sigma$. The exponential probability density, p, is given by:

$$p(x) = \exp(-x/\mu)/\mu \tag{67}$$

The Ricean density for the signal amplitude is:

$$p(x) = \frac{x}{\sigma^2} \exp\left(-\frac{x^2 + v^2}{2\sigma^2} \right) I_0\left(\frac{xv}{\sigma^2} \right) \tag{68}$$

Here v is the amplitude of the signal from the direct path and σ^2 corresponds to a Rayleigh distributed noisy component from the other paths. The function, I_0, is a modified Bessel function of the first kind of order zero. When $v = 0$, the Ricean density goes to the Rayleigh density. The problem with the Ricean density is that it requires two parameters, neither of which may be easy to predict.

The Nagakami-m density for the signal amplitude is:

$$p(x) = \frac{2(m/\sigma^2)^m x^{2m-1}}{\Gamma(m)} \exp\left(-\frac{mx^2}{\sigma^2} \right) \tag{69}$$

where σ^2 is now the mean square amplitude and the parameter m is called the "fading figure". Again there are two parameters, which may be difficult to predict.

As shown in [4], the effects of phase variations depend on the relative magnitudes of the fading correlation time and either the reciprocal of the channel coherence bandwidth or the symbol duration. If the correlation time is very large, the variations in phase can be regarded as slow and the effect will be the same over the entire frequency spectrum of the signal. Also the phase will be roughly constant over each symbol. This leads to a classification in which there are four categories: Flat-Flat, Frequency-Flat, Time-Flat and Non-Flat.

For AIS signals, which are based on GMSK modulation, the 3 dB bandwidth is significantly smaller than 10 kHz (Graphs for GMSK spectra are provided in [4]). The bit rate is 9600 bit/s so that the symbol interval is about 0.1 ms. Ships travel at velocities up to 10 m/s and the wavelength of AIS transmissions is about 1 m; the Doppler shifts are up to 10 Hz and the correlation time can be expected to be of the order of the reciprocal of this, namely 0.1 s. Therefore we expect multi-path to be Flat-Flat except under special circumstances (e.g. reflections from aircraft, significant tropospheric scatter as described in [21] and [26] as well as high winds and sea states). This implies that fading is usually slow and the principal concern is insufficient received power. The conclusion is consistent with a statement in [21].

The effect of multi-path depends somewhat on the receiver. A table and graphs are provided in [4] and [33] for the coherent and non-coherent FSK systems. It is shown that, in terms of Bit Error Rate (BER), the performance of coherent detection is better than non-coherent detection in the presence of Flat-Flat fading. However, though modern AIS transponders typically use coherent detection, older models are usually based on non-coherent detection[9].

In summary, multi-path depends on how a transmitting ship's antenna is mounted, the ship superstructure, the wind speed, which can drive a thin layer of water at speeds approaching the wind speed, and the receiver configuration, including antenna height and surrounding terrain. The way in which the signals are demodulated in the receiver affects the detected signals. Any

[9] From a conversation with the terrestrial AIS transponder design firm Fidus, Ottawa.

rapid changes in the path characteristics may result in rapid fading, which can be represented as a loss of signal. The best modeling solution is to employ existing simple general algorithms and expressions that are based on practical experience [26].

For example, in [21] the following expression is used for the trans-horizon multi-path loss, L, in decibels:

$$L = 2.6\left[1 - \exp(-0.1d)\right]\log_{10}(\beta / 50) \tag{70}$$

where d is the total path length in kilometres and β is the probability that the loss is not exceeded as a percentage. For example, if d = 50 km or more, the exponential term is negligible and a loss of 1.8 dB will be exceeded for 10% of the time; a loss of 4.4 dB will be exceeded for 1% of the time. This at least provides an order of magnitude of the loss to be expected in spite of the large number of unknowns and parameters that are difficult to predict in practice.

Propagation Over Land

The propagation of AIS signals is affected when obstacles obscure the direct line of sight to the ship. However, it may still be possible to receive the AIS signals because they are diffracted around an obstacle, though there may be very large losses. The presence of an obstacle close to the line of sight path can cause a loss but it can also result in an increase in the signal; again this is due to diffraction effects. In the case of land, the obstacle may be a hill and for a ship it could be part of the ship's superstructure.

There are several models for diffraction. The simplest can be understood in terms of the Huygens construction of wave fronts. This type of approximation is due to Fresnel and is a scalar model of electromagnetic propagation; it is incapable of handling polarization effects. Though it is easy to obtain results for simple geometries, such as an occluding disc or knife edge, it is more difficult to apply it more generally in three dimensions.

Maxwell's equations, which describe electromagnetic wave propagation, are vector equations. Direct solutions of these equations for practical problems are far too computationally intensive because the region of scattering must be represented to a resolution better than one half wavelength. Therefore approximation is needed. In many cases the vector equations may be reduced to scalar equations. This is valid if the geometry allows the electric or magnetic vector to lie always along one coordinate axis. This applies in two-dimensional problems. In some cases, for example when a scatterer is infinitely conducting, the reflection coefficient is independent of polarization. Then, scalar models can be applied successfully. Problems may occur when the scatterers have finite conductivity and when there is significant cross-polarization of the signals during the scattering process.

The reality is that, when an electromagnetic wave is incident upon a scatterer, the scatterer blocks part of the wavefront and excites currents in it; these latter reradiate energy. The calculation of these currents requires boundary conditions to be solved and this is usually quite difficult, especially if there is a need to obtain results in closed form. Solutions have only been achieved for a few canonical cases, such as the semi-infinite plane and the wedge [35], and then only when the wavelength is small compared to the size of the object. However, this covers many practical

cases. Small wavelength approximation theory is the domain of ray theory; other models are based on this. One advantage of some ray theories is that they can handle polarization.

The Geometric Theory of Diffraction (GTD) was developed by Keller [36] and is valid as the wavelength goes to zero compared with the other dimensions. The diffracted rays are just like any other rays and the only difficulty is the determination of the initial field at the point of diffraction. The theory provides this as a factor by which the incident ray is multiplied on diffraction. As noted, canonical models are used to assist in representing real objects. These are based on some exact solutions and include the vertex of an edge and the tip of a cone. Unfortunately GTD tends to fail near to the shadow boundary.

The Uniform Theory of Diffraction (UTD) is another ray model, which is more accurate. However, both GTD and UTD can be difficult to apply partly because the scattering factors are quite complicated compared with Fresnel diffraction but mostly because the calculation of all possible ray paths may be difficult. The presence of caustics, where rays coalesce and the signal amplitude goes to infinity, can also cause complications.

In practice, the diffraction of radio signals is often treated with sufficient accuracy by Fresnel diffraction. This is partly because diffraction by terrain, buildings, etc. involves a number of uncertainties, such as the conductivity of the material and the shape of the scatterer, which is usually not known to within a fraction of a wavelength.

A useful review of GTD and some UTD is provided in [37].

Diffraction losses are discussed by Hall [16] and Barclay [2]. It is assumed that the obstacle is in the far field of both transmitting and receiving antennas so that the Fresnel approximation to diffraction applies; the treatment is in terms of Fresnel zones and the simplest case is knife-edge diffraction. Once the geometry has been established, the Fresnel zones, which are contours of constant phase, can be calculated. Determination of the signal strength consists of integrating the complex amplitudes over the aperture left unobscured by the obstacle. The integrals for a straight edge are of the form (Fresnel integrals):

$$I(v) = \int_0^v \exp\left(i\frac{\pi x^2}{2} \right) dx \tag{71}$$

When v goes to infinity, the integral $I(\infty) = 0.5 + i0.5$; in between $-\infty$ and ∞, we have a Cornu spiral. To evaluate the diffraction from a straight edge, which is a two-dimensional problem we need:

$$\int_v^\infty \exp\left(i\frac{\pi x^2}{2} \right) dx \tag{72}$$

This yields the familiar diffraction pattern, which exhibits oscillations at points clear of obstruction and tapers off rapidly in the shadow. Near the shadow boundary there is about a 6 dB loss in the power. Therefore it is important in the design of terrestrial communications systems to leave sufficient clearance of the direct path above any obstacle. This needs to take into account

any effects of tropospheric refraction effects, such as ducting. In practice the loss, L, in the region of attenuation can be approximated by [2]:

$$L = 6.9 + 20.0 \log_{10}\left(\sqrt{(\nu - 0.1)^2 + 1} + \nu - 0.1\right) \tag{73}$$

For example, if the path from transmitter to hilltop is of length d_1 and that from hilltop to receiver is d_2, and the hill is represented as a knife edge of height h above the direct path, and the loss is given by (73), then v is given by:

$$\nu = h\sqrt{\frac{2}{\lambda}\left(\frac{1}{d_1} + \frac{1}{d_2}\right)} \tag{74}$$

It is pointed out by Barclay [2] that the clearance required to avoid attenuation from diffraction on point-to-point links corresponds to a value of v = -0.85.

When there is a sequence of diffracting obstacles, the signal may be estimated using a method of Deygout [38]. This method starts by identifying the most prominent obstacle that gives the greatest value of v. Diffraction loss is calculated for this obstacle alone. Then the path is subdivided for the next most prominent obstacle and the process is repeated to determine a further loss, which is added (in decibels) to the first. This is then repeated until all obstacles are taken into account.

Diffraction Over Sea

On VHF trans-horizon paths, diffraction takes place over the earth's surface. This extends the path beyond the cut-off implied by geometric optics. The extent to which the path length is increased depends on the signal power, the curvature of the earth, tropospheric refraction, the wavelength and the sensitivity of the receiver. The topic has been discussed by Ekstrom [39] and is applicable to smooth terrain, such as the sea. The loss is expressed as a reduction factor, F, on the electric field.

Normalized distances X and Z are defined by:

$$\begin{aligned} X &= 0.7937d\left(\frac{2\pi}{\lambda}\right)^{1/3}\left(kr_e\right)^{-2/3} \\ Z &= 1.26h\left(\frac{2\pi}{\lambda}\right)^{2/3}\left(kr_e\right)^{-1/3} \end{aligned} \tag{75}$$

where d is the distance, h is the antenna height, λ is the wavelength, r_e is the earth radius, all in metres, and k is the refractive-gradient earth-radius factor, which is nominally 4/3.

The reduction factor is given by:

$$F = V(X)\,|\,U(Z_T)\,||\,U(Z_R)\,| \tag{76}$$

where the subscripts T and R denote transmitter and receiver respectively and:

$$
\begin{aligned}
V(X) &= 2\sqrt{\pi X}\exp\left(-2.025X\right) \\
|U(Z)| &= Z\sqrt{1+\frac{1}{(hl)^2}+\frac{2}{hl}\sin\phi} \\
l &= \sqrt{\frac{2\pi\, p}{\lambda}} \\
p &= \frac{2\pi}{\lambda}\frac{\left[(\varepsilon-1)^2+(60\sigma\lambda)^2\right]^{1/2}}{\left[\varepsilon^2+(60\sigma\lambda)^2\right]^b}
\end{aligned}
\tag{77}
$$

Here $b = 0$ for horizontal polarization and $b = 1$ for vertical polarization. Also ε is the relative permittivity of the surface material (typically the sea), σ is its conductivity in mho/m and:

$$
\begin{aligned}
\phi &= \frac{\pi}{4}-\frac{1}{2}\tan^{-1}\frac{\varepsilon-1}{60\sigma\lambda} \quad \text{horizontal polarization} \\
\phi &= \frac{5\pi}{4}+\frac{1}{2}\tan^{-1}\frac{\varepsilon-1}{60\sigma\lambda} \quad \text{vertical polarization}
\end{aligned}
\tag{78}
$$

The range of validity is limited to distances larger than that of the sum of the radio horizons, taking into account the curvature of the earth modified by refractivity gradients. This propagation distance according to geometric optics and taking into account the refractivity is given by:

$$
d_{GO} = \sqrt{2kr_e}\left(\sqrt{h_T}+\sqrt{h_R}\right) \tag{79}
$$

Using the parameters in Table 7, it turns out to be 38.6 km. There are also some other formal conditions that are usually satisfied for AIS signals but this should be verified by referring to [39].

Figure 6 shows the loss as a function of range for AIS signals as a function of range calculated from the above equations[10]. AIS signals are vertically polarized, the refractivity coefficient for the earth radius is assumed to have the standard value and the heights of the antennas are 15 m for the ship and 30 m for the shore based receiver. The parameters, some of which are from [39], are provided in Table 7.

Table 7: Parameters for Diffraction Loss

Polarization	Vertical
Receiving Antenna Height (m)	30
Transmitting Antenna Height (m)	15
Earth Radius (km)	6400
Refractivity Coefficient, k	4/3
Relative Permittivity	81
Conductivity (mho/m)	4
Frequency (MHz)	162
Transmit Power (W)	12.5

[10] Numerical examples in [39] were used to verify a spreadsheet calculation.

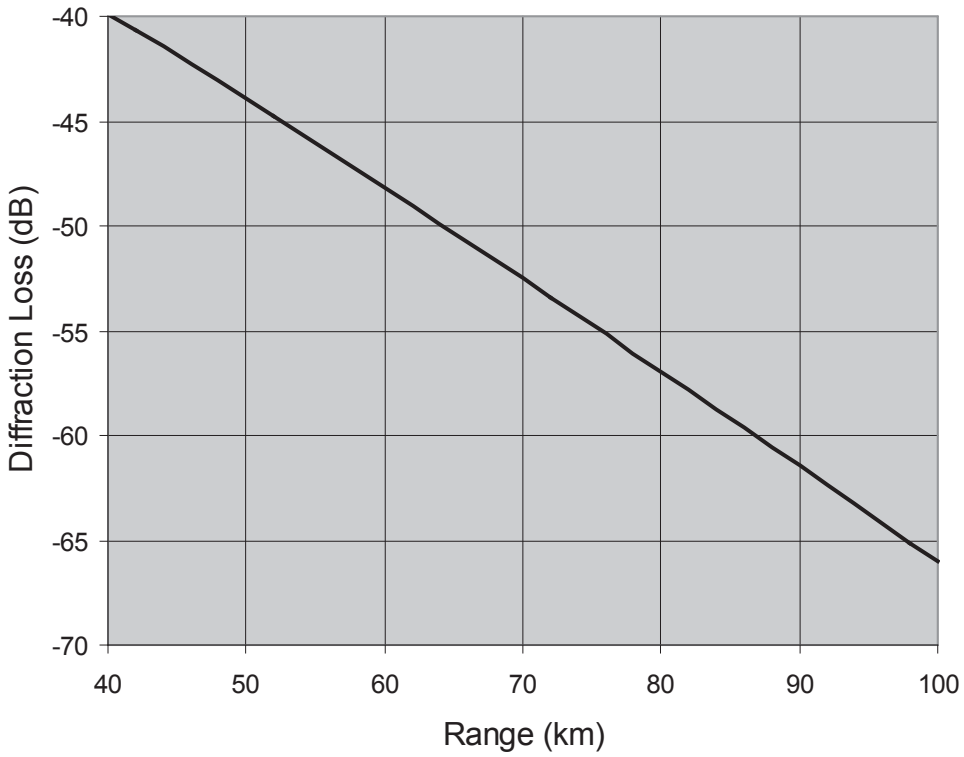

Figure 6: Loss due to refraction around the earth

The minimum sensitivity of an AIS receiver, as specified by the ITU, is -107 dBm. The power, P_R, received from a Class A transmitter at an unobstructed range r is given by:

$$P_R = \frac{G_T G_R P_T \lambda^2}{(4\pi r)^2} \tag{80}$$

where $G_{T,R}$ are the antenna gains. Therefore when the antennas are isotropic, the unobstructed received power at a range of 50 km would be about -69 dBm. This is reduced by diffraction to about -112 dBm and so would be just below the nominal detection threshold of the receiver. Therefore we can conclude that diffraction over the sea around the curvature of the earth is significant in extending the range of AIS signals. It should be taken into account in AIS signal modeling.

ITU Model Applied to AIS

The ITU has published a model for VHF propagation in the form of a spreadsheet containing Visual Basic codes. The model implements the ITU Recommendation ITU-R P.452-14 [26]. This can be applied to AIS signals though it is aimed at predicting the interference from extraneous signals.

The recommendation applies to signals at frequencies above 100 MHz and permits the propagation losses to be estimated over line of sight as well as trans-horizon paths. It includes diffraction over a smooth earth, diffraction over obstacles, tropospheric scatter, ducting (including elevated ducts) and hydrometeor scatter.

Predictions can be made for yearly average propagation or worst month. A key parameter is the probability that the loss will not be exceeded. This is the same as the probability that the signal strength of a desired signal is greater than the calculated value. Alternatively, the calculations can be interpreted in terms of the probability that a signal can be received from a certain range, though some iteration may be needed.

The basic input data, which is entered in Step 1, is shown in Table 8. The inputs are in the yellow boxes and refer to AIS signals off the east coast of Canada.

Table 8: Input Data

Parameter	User input	Preferred resolution	Description
f	**0.161**	0.01	Frequency (GHz)
p	**10**	0.001	Required time percentage(s) for which the calculated basic transmission loss is not exceeded (%)
φ_t	**45.0**	0.001	Latitude of transmitting (interfering) station (degrees)
ψ_t	**-62.0**	0.001	Longitude of transmitting (interfering) station (degrees)
φ_r	**45.0**	0.001	Latitude of receiving (interfered-with) station (degrees)
ψ_r	**-63**	0.001	Longitude of receiving (interfered-with) station (degrees)
h_{tg}	**15**	1	Transmitting antenna centre height above ground level (m)
h_{rg}	**15**	1	Receiving antenna centre height above ground level (m)
G_t	**2**	0.1	Transmitting antenna gain in the direction of the horizon along the great-circle interference path (dBi)
G_r	**2**	0.1	Receiving antenna gain in the direction of the horizon along the great-circle interference path (dBi)

The latitudes and longitudes are only used to estimate the variability of the refractive index lapse rate and do not determine the range of the signal. Therefore they do not have to be specified accurately.

Following this in Step 2, it is necessary to specify whether the calculation is for a yearly average loss or for a worst month loss. If the latter is required, it is necessary to enter the fraction of the path that is over water.

In Step 3, two parameters are entered. The first is the average refractive index lapse rate through the lowest 1 km of the atmosphere. This can be established by referring to Figure 11 of the spreadsheet, which provides a world map with contours of average refractivity lapse rate. Alternatively the maximum mean values of refractive index lapse rate are in Figure 12 for the worst month predictions. The second parameter is the surface refractivity and this can be found in Fig. 13.

In Step 3b, data is entered to resolve an ambiguity in the theory. Entries are only needed when the path is over water, which will be the case when the application is to AIS. However, because paths of less than 5 km in length are of little interest here, a large value (e.g., 500 km) can be entered into the first box and this can serve as a default value.

Step 4 is the terrain profile analysis. The first column represents range. It is important to note that the final row in this sheet gives the ground range of the transmitter. The second column represents the height of the terrain over the mean sea level. For paths over the sea, this takes the value zero. The third column represents the radio-climatic zone as shown in Table 9.

Table 9: Radio-climatic zones

Zone Type	Code	Definition
Coastal Land	A1	Coastal land and shore areas, i.e., land adjacent to the sea up to an altitude of 100 m relative to mean sea or water level, but limited to a distance of 50 km from the nearest sea area. Where precise 100 m data are not available an approximate value, i.e. 300 ft, may be used
Inland	A2	All land, other than coastal and shore areas defined as “coastal land” above
Sea	B	Seas, oceans and other large bodies of water (i.e. covering a circle of at least 100 km in diameter)

The test profile sheet in the spreadsheet should be examined to verify that all data has been entered correctly and that the numbers are reasonable.

As an example we can use the data in Table 8 to calculate the loss over the sea over a range of 120 km. For 10% of the time, the loss will not be any greater than what is calculated. This entails using 120 entries in Step 4 spaced at intervals of 1 km with heights of zero. The radio-climatic zone is ‘B’ for all entries in the third column. When the Calculate button is clicked, the average yearly loss is 150.5 dB. If the worst month analysis is needed, Step 3 is changed and the

fraction of the path over sea is entered as '1'. The result is 141.3 dB. This is a smaller loss and indicates a higher signal level by 9.2 dB.

The analysis of AIS can be completed by comparing the received signal strength with the specified AIS receiver sensitivity of -107 dBm. The path loss calculated by the spreadsheet, L_p, is related to the received signal strength, P_R, by:

$$P_R = G_R G_T P_T L_p \tag{81}$$

where P_T is the transmitter power and $G_{R,T}$ are the antenna gains. If the antenna gains are each 2 dB, the transmitter power is 12.5 W (41 dBm) and the path loss is 150.5 dB, the received signal is -105.5 dBm. This is higher than the lower limit of -107 dBm and therefore the AIS signal will be detectable for over 10% of the time even over a path length of 120 km.

The Visual Basic codes are visible by typing (ALT)-(F11) and may be copied. Otherwise access to the spreadsheet is restricted by password protection.

Conclusions

The literature review has summarized a number of phenomena which may affect VHF propagation, and hence the transmission of AIS signals. These phenomena can have the effect of producing interference signals, and can also have the effect of extending the signal range beyond the line-of-sight.

Three phenomena were determined most likely to have a significant effect on AIS transmission.

- Diffraction over the sea around the curvature of the earth, as outlined in section 6.3, is significant in extending the range of AIS signals and should be considered.
- Ducting resulting from the varying refractivity of air, as outlined in section 4.2, can also extend the transmission range.
- Multipath effects can cause significant variability in the received signal strength. These effects are principal components of the ITU Recommendation ITU-R P.452-14 [26].

Two other components of ITU-R P.452-14—tropospheric scatter and scatter from hydrometeors—were not found, based on the calculations in section 4.1 and section 4.4 respectively, to have a significant effect in extending the transmission range of typical AIS signals.

The other effects considered, notably scattering resulting from ionospheric layers, meteor trails, and lightning, were deemed to be unlikely to either cause interference or extend the transmission range of AIS signals.

Based on these findings, it is recommended that the software implementation of ITU-R P.452-14, available in [22], be considered for modelling the mentioned VHF propagation effects in the context of AIS transmissions.

References

[1] "Technical Characteristics for an Automatic Identification System using Time-Division Multiple Access in the VHF Maritime Mobile Band," International Telecommunications Union 2010.

[2] L. Barclay, *Propagation of Radio Waves*, 2nd ed. London, United Kingdom: The Institution of Electrical Engineers, 2003.

[3] A. Harati-Mokhtari*, et al.*, "Automatic Identification System (AIS): A Human Factors Approach," *Journal of Navigation,* vol. 60, pp. 373-389, 2007.

[4] S. Haykin, *Communications Systems*, 4th ed.: John Wiley & Sons, Inc., 2001.

[5] M. Hall and L. Barclay, *Radiowave Propagation*. London, United Kingdom: Peter Peregrinus Ltd., 1989.

[6] L. Boithias, *Radio Wave Propagation*. London, United Kingdom: North Oxford Academic Publishers Ltd, 1987.

[7] V. I. Tatarski, *Wave Propagation in a Turbulent Medium*. New York: McGraw-Hill, 1961.

[8] B. I. Bleaney and B. Bleaney, *Electricity and Magnetism*: Oxford University Press, 1959.

[9] P. Debye, *Polar Molecules*: Dover, 1929.

[10] E. K. Smith and S. Weintraub, "The Constants in the Equation for Atmospheric Refractive Index at Radio Frequencies," *Proceedings of the IRE,* pp. 1035-1037, 1953.

[11] M. H. Bataineh and C. V. Macario, "Modelling Refractivity Variation in the VHF/UHF Bands," *Communications,* vol. 1, pp. 267-271, 1996.

[12] G. Birnbaum and S. K. Chatterjee, "The Dielectric Constant of Water Vapor in the Microwave Region," *Journal of Applied Physics,* vol. 23, pp. 220-223, February 1952.

[13] B. Edlén, "The refractive index of air," *Metrologia,* vol. 1, pp. 71-80, 1966.

[14] K. P. Birch and M. J. Downs, "An Updated Edlen Equation for the Refractive Index of Air," *Metrologia,* vol. 30, pp. 155-162, 1993.

[15] K. P. Birch and M. J. Downs, "Correction to the Updated Edlen Equation for the Refractive Index of Air," *Metrologia,* vol. 31, pp. 315-316, 1994.

[16] M. P. M. Hall, *Effect of the Troposphere on Radio Communications*. London, United Kingdom: Peter Peregrinus Ltd., 1979.

[17] W. K. Prusaczyk, "Precise Water Vapor Pressure Value Calculations," *Computers and Biomedical Research,* vol. 19, pp. 129-130, 1989.

[18] R. Reid*, et al.*, *The Properties of Gases and Liquids*, 4th ed.: McGraw-Hill, 1987.

[19] C. L. Yaws and H. C. Yang, "To Estimate Vapor Pressure Easily," *Hydrocarbon Processing,* vol. 68, pp. 65-68, 1989.

[20] P. E. Ciddor, "Refractive Index of Air: New Equations for the Visible and Near Infrared," *Applied Optics,* vol. 35, pp. 1566-1573, March 1996.

[21] "Propagation Prediction Techniques and Data Required for the Design of Trans-Horizon Radio-Relay Systems," International Telecommunications Union ITU-R P.452-14, 1992.

[22] ITU. *Point to Point (Interference) Propagation (Rec. P452)*. Available: http://www.itu.int/ITU-R/index.asp?category=study-groups&rlink=rsg3-software-ionospheric&lang=en

[23] M. Levy, *Parabolic equation methods for electromagnetic wave propagation*. London, United Kingdom: The Institution of Electrical Engineers, 2000.

[24] N.-H. Jeong and J.-K. Pack, "Statistical Modeling of Atmospheric Refractivity for Ducting Channel from Meteorological Observation Data in Marine Environments," presented at the 2003 Asia-Pacfic Conference on Applied Electromagnetics (APACE 2003), Shah Alam, Malaysia, 2003.
[25] G. Hauser. *Propagation*. Available: http://www.anarc.org/wtfda/propagation.htm
[26] "Prediction Procedure for the Evaluation of Interference between Stations on the Surface of the Earth at Frequencies above about 0.1 GHz," International Telecommunications Union ITU-R P.452-14, 2009.
[27] K. Davies, *Ionospheric Radio*. London, United Kingdom: Peter Peregrinus Ltd., 1990.
[28] D. K. Bailey*, et al.*, "Radio Transmission at VHF by Scattering and Other Processes in the Lower Ionosphere," *Proceedings of the IRE,* vol. 43, pp. 1181-1230, 1955.
[29] R. M. Davis*, et al.*, "Sporadic E at VHF in the USA," in *Proc. IRE*, 1959, p. 762.
[30] H. Dazhang*, et al.*, "Model of Es Occurrence Probability in China at 1985-2006," in *4th International Symposium on Electromagnetic Compatibility*, 2007.
[31] L. V. Blake, *Radar Range Performance*: Artech House, 1986.
[32] E. F. Knott*, et al.*, *Radar Cross Section*: Artech House, 1985.
[33] J. G. Proakis, *Digital Communications*, 4th ed.: McGraw-Hill, 2001.
[34] W. Feller, *An Introduction to Probability Theory and Its Applications, Vol. II*: J. Wiley & Sons, Inc., 1971.
[35] R. G. Kouyoumjian, "Asymptotic High-Frequency Methods," *Proc. IEEE,* vol. 53, pp. 864-876, August 1965.
[36] J. B. Keller, "Geometrical Theory of Diffraction," *J. Opt. Soc. America,* vol. 52, pp. 116-130, 1962.
[37] R. C. Hansen, *Geometrical Theory of Diffraction*: IEEE Press, 1981.
[38] J. Deygout, "Multiple Diffraction of Microwaves," *IEEE Trans. Antennas Propagation,* vol. AP-14, p. 480, 1966.
[39] J. L. Ekstrom, "VHF-UHF Propagation Performance Predictions for Low Altitude Communication Links Operating Over Water," in *Proceedings of the IEEE Mililtary Communications Conference*, 1993, pp. 605-608.

List of symbols/abbreviations/acronyms/initialisms

AES	Advanced Encryption Standard
AIS	Automatic Identification of Ships
AWGN	Additive White Gaussian Noise
BER	Bit Error Rate
CISTI	Canada Institute for Scientific and Technical Information
CSTDMA	Carrier Sense Time Domain Multiple Access
DFSK	Differential Frequency Shift Keying
DND	Department of National Defence
DPSK	Differential Phase Shift Keying
DRDC	Defence Research & Development Canada
DRDKIM	Director Research and Development Knowledge and Information Management
ETA	Estimated Time of Arrival
FSK	Frequency Shift Keying
GMSK	Gaussian Minimum Shift Keying
GTD	Geometric Theory of Diffraction
IALA	International Association of Lighthouse Authorities
IEEE	Institute of Electrical and Electronics Engineers
IMO	International Maritime Organization
ITU	International Telecommunications Union
LRDC	London Research and Development Corporation
MMSI	Maritime Mobile Service Identity
MSK	Minimum Shift Keying
NRZI	Non Return to Zero Inverted
PER	Packet Error Rate
QPSK	Quadrature Phase Shift Keying
R&D	Research & Development
RCS	Radar Cross Section
RF	Radio Frequency
RFP	Request For Proposal

SNR	Signal-to-Noise Ratio
SOLAS	Safety Of Life At Sea
SOTDMA	Self-Organized Time Domain Multiple Access
TDMA	Time Domain Multiple Access
UTD	Uniform Theory of Diffraction
VHF	Very High Frequency

Distribution list

Document No.: DRDC Atlantic CR 2011-152

LIST PART 1: Internal Distribution by Centre

1 F. DESHARNAIS
1 M. MCINTYRE
1 T. HAMMOND
2 A.W. ISENOR (1 CD, 1 hard copy)
1 S. WEBB
1 A. MACINNIS
1 D. SCHAUB
1 L. LAPINSKI
3 DRDC Atlantic Library (1 hard copy, 2 CDs)

12 TOTAL LIST PART 1

LIST PART 2: External Distribution by DRDKIM

1 Library and Archives Canada, Atten: Military Archivist, Government Records Branch

1 NDHQ/DRDKIM 2-2-5

1 Stéphane Paradis
DRDC Valcartier
2459 Pie-XI Blvd North, Québec, QC G3J 1X5

1 Andrew Wind, DRDC CORA
MARLANT HQ
3rd Floor, Room 311
PO Box 99000 Stn Forces, Halifax, NS B3K 5X5

1 C-CORE
1 Morrissey Road, St. John's, NL A1B 3X5
Attn: Chris Fowler

1 Commanding Officer
TRINITY JOSIC, PO Box 99000 Stn Forces, Halifax, NS B3K 5X5

1 Commanding Officer
OIC Maritime Operations Centre, JTFP HQ
MARPAC/JTFP, PO Box 17000 Station Forces, Victoria, BC B9A 7N2

7 TOTAL LIST PART 2

19 TOTAL COPIES REQUIRED

This page intentionally left blank.

DOCUMENT CONTROL DATA

(Security classification of title, body of abstract and indexing annotation must be entered when the overall document is classified)

1. ORIGINATOR (The name and address of the organization preparing the document. Organizations for whom the document was prepared, e.g. Centre sponsoring a contractor's report, or tasking agency, are entered in section 8.)

C-CORE
1 Morrissey Road
St. John's, NL
A1B 3X5

2. SECURITY CLASSIFICATION (Overall security classification of the document including special warning terms if applicable.)

UNCLASSIFIED
(NON-CONTROLLED GOODS)
DMC A
REVIEW: GCEC JUNE 2010

3. TITLE (The complete document title as indicated on the title page. Its classification should be indicated by the appropriate abbreviation (S, C or U) in parentheses after the title.)

VHF Propagation Study

4. AUTHORS (last name, followed by initials – ranks, titles, etc. not to be used)

Green D.; Tunaley J. K. E.; Fowler C.; Power D.

5. DATE OF PUBLICATION (Month and year of publication of document.)

September 2011

6a. NO. OF PAGES (Total containing information, including Annexes, Appendices, etc.)

62

6b. NO. OF REFS (Total cited in document.)

39

7. DESCRIPTIVE NOTES (The category of the document, e.g. technical report, technical note or memorandum. If appropriate, enter the type of report, e.g. interim, progress, summary, annual or final. Give the inclusive dates when a specific reporting period is covered.)

Contract Report

8. SPONSORING ACTIVITY (The name of the department project office or laboratory sponsoring the research and development – include address.)

Defence R&D Canada – Atlantic
9 Grove Street
P.O. Box 1012
Dartmouth, Nova Scotia B2Y 3Z7

9a. PROJECT OR GRANT NO. (If appropriate, the applicable research and development project or grant number under which the document was written. Please specify whether project or grant.)

11hl; 11ho

9b. CONTRACT NO. (If appropriate, the applicable number under which the document was written.)

W7707-115279

10a. ORIGINATOR'S DOCUMENT NUMBER (The official document number by which the document is identified by the originating activity. This number must be unique to this document.)

R-11-020-868

10b. OTHER DOCUMENT NO(s). (Any other numbers which may be assigned this document either by the originator or by the sponsor.)

DRDC Atlantic CR 2011-152

11. DOCUMENT AVAILABILITY (Any limitations on further dissemination of the document, other than those imposed by security classification.)

Unlimited

12. DOCUMENT ANNOUNCEMENT (Any limitation to the bibliographic announcement of this document. This will normally correspond to the Document Availability (11). However, where further distribution (beyond the audience specified in (11) is possible, a wider announcement audience may be selected.))

Unlimited

13. ABSTRACT (A brief and factual summary of the document. It may also appear elsewhere in the body of the document itself. It is highly desirable that the abstract of classified documents be unclassified. Each paragraph of the abstract shall begin with an indication of the security classification of the information in the paragraph (unless the document itself is unclassified) represented as (S), (C), (R), or (U). It is not necessary to include here abstracts in both official languages unless the text is bilingual.)

This literature review provides DRDC researchers with information related to the propagation of VHF signals, particularly as it relates to the fluctuating limits of Automatic Identification System (AIS) message reception. The review focuses on the AIS frequency range and the factors that influence signal propagation in Maritime environments. The approach taken was consultation with classical textbooks on propagation to capture fundamental equations, followed by a search of the literature for papers involving VHF propagation of AIS signals. Three effects were determined to most likely extend the range of AIS transmission: diffraction over the sea around the curvature of the earth, ducting resulting from the varying refractivity of air

La présente revue de littérature fournit aux chercheurs de RDDC des renseignements sur la propagation des signaux VHF, particulièrement en ce qui concerne les limites fluctuantes de réception de messages du Système d'identification automatique (AIS). Elle porte surtout sur la gamme de fréquences de l'AIS et les facteurs qui influencent la propagation des signaux en milieu maritime. L'approche utilisée a consisté à d'abord consulter des manuels classiques sur la propagation afin de relever les équations fondamentales, puis à effectuer des recherches dans les publications scientifiques pour trouver des articles portant sur la propagation des signaux AIS. Ce travail a permis de déterminer que trois effets étendent très vraisemblablement la portée de transmission AIS : la diffraction sur la surface de la mer en raison de la courbure terrestre, la propagation guidée résultant de la variation de l'indice de réfraction de l'air, et les effets des trajets multiples.

14. KEYWORDS, DESCRIPTORS or IDENTIFIERS (Technically meaningful terms or short phrases that characterize a document and could be helpful in cataloguing the document. They should be selected so that no security classification is required. Identifiers, such as equipment model designation, trade name, military project code name, geographic location may also be included. If possible keywords should be selected from a published thesaurus, e.g. Thesaurus of Engineering and Scientific Terms (TEST) and that thesaurus identified. If it is not possible to select indexing terms which are Unclassified, the classification of each should be indicated as with the title.)

VHF; AIS; Automatic Identification System; Very High Frequency

This page intentionally left blank.

Defence R&D Canada

Canada's leader in defence
and National Security
Science and Technology

R & D pour la défense Canada

Chef de file au Canada en matière
de science et de technologie pour
la défense et la sécurité nationale

DEFENCE DÉFENSE

www.drdc-rddc.gc.ca